arXiv:astro-ph/0505149v2 15 May 2005

# Pulsation and evolutionary masses of classical Cepheids. I. Milky Way variables

F. Caputo [1], G. Bono [1], G. Fiorentino [1,2], M. Marconi [3], I. Musella [3]

*1. INAF − Osservatorio Astronomico di Roma, Via Frascati 33, 00040 Monte Porzio Catone, Italy; caputo@mporzio.astro.it; bono@mporzio.astro.it*

*2. Università di Roma Tor Vergata, via della Ricerca Scientifica 1, 00133 Roma, Italy; giuliana@mporzio.astro.it*

*3. INAF − Osservatorio Astronomico di Capodimonte, Via Moiariello 16, 80131 Napoli, Italy; marcella@na.astro.it; ilaria@na.astro.it*

## ABSTRACT

We investigate a selected sample of Galactic classical Cepheids with available distance and reddening estimates in the framework of the theoretical scenario provided by pulsation models, computed with metal abundance $Z$=0.02, helium content in the range of $Y$=0.25 to 0.31, and various choices of the stellar mass and luminosity. After transforming the bolometric light curve of the fundamental models into $BVRIJK$ magnitudes, we derived analytical relations connecting the pulsation period with the stellar mass, the mean (intensity-averaged) absolute magnitude, and the color of the pulsators. These relations are used together with the Cepheid observed absolute magnitudes in order to determine the "pulsation" mass -$M_p$- of each individual variable. The comparison with the "evolutionary" masses -$M_{e,can}$- given by canonical (no convective core overshooting, no mass-loss) models of central He-burning stellar structures reveals that the $M_p/M_{e,can}$ ratio is correlated with the Cepheid period, ranging from $\sim$ 0.8 at log$P$=0.5 to $\sim$ 1 at log$P$=1.5. We discuss the effects of different input physics and/or assumptions on the evolutionary computations, as well as of uncertainties in the adopted Cepheid metal content, distance, and reddening. Eventually, we find that the pulsational results can be interpreted in terms of mass-loss during or before the Cepheid phase, whose amount increases as the Cepheid original mass decreases. It vanishes around $13M_{\odot}$ and increases up to $\sim$ 20% at $4M_{\odot}$.

## 1. Introduction

Classical Cepheids have long been recognized as primary standard candles to estimate the distance of external galaxies out to the Virgo cluster. Moreover, through the calibration

of secondary distance indicators, they allow the investigation of even more remote stellar systems, thus enabling us to obtain information on the Hubble constant (Ferrarese et al. 2000; Freedman et al. 2001; Saha et al. 2001). However, their importance exceeds the determination of distances, since they are powerful astrophysical laboratories providing fundamental clues for studying the evolution of intermediate-mass stars and, in particular, the occurrence of mass-loss along the Red Giant (RG) and the central He-burning evolutionary phases.

From the point of view of the stellar evolution theory, Cepheids are indeed generally interpreted as post-RG stars crossing the pulsation region of the HR diagram during the characteristic "blue loop" connected with core He-burning. During this phase, the luminosity $L$ of the evolutionary track mainly depends on the original stellar mass $M$ and the chemical composition: therefore, the evolutionary models computed by neglecting the mass-loss, provide a Mass-Luminosity ($ML$) relation, which is widely used to estimate the "evolutionary" mass of Cepheids for which absolute magnitudes and chemical composition are available. On the other hand, the Cepheid pulsation period depends, at fixed chemical composition, on the star mass, luminosity and effective temperature, hence the ensuing mass-dependent Period-Luminosity-Color ($PLC$) relation can be used to estimate the "pulsation" mass of each individual variable with known metal content, absolute magnitude and intrinsic color. With a slightly different approach, the theoretical Period-Mass-Radius ($PMR$) relation can be applied to Cepheids for which accurate estimates of radii are available.

In the last decades, a large amount of work has been devoted to the comparison between pulsation and evolutionary masses, leading to the long-debated problem of the "Cepheid mass discrepancy" (see Cox 1980). Almost all the studies suggest that the pulsation masses are smaller than the evolutionary ones, but the amount of such a discrepancy has not been firmly established. Among the most recent papers, we recall Bono et al. (2001, hereafter B01) and Beaulieu et al. (2001, hereafter BBK), who studied Cepheids in the Galaxy and in the Magellanic Clouds, respectively.

By relying on a sample of 31 variables with accurate radii, distances and photometric parameters, B01 used theoretical $PMR$ relations neglecting the width in temperature of the instability strip in order to determine the pulsation mass $M_p$. From the comparison with evolutionary masses $M_{e,can}$ inferred by canonical (i.e., no mass-loss, no convective core overshooting) evolutionary tracks, they show that the ratio between $M_p$ and $M_{e,can}$ varies from 0.8 to 1, with a feeble evidence for an average discrepancy of the order of $\sim 13\%$ for short-period Cepheids and $\sim 10\%$ for long-period ones (see also Gieren 1989). A similar comparison was also performed by BBK, who investigated the huge OGLE database of Magellanic Cepheids (Udalski et al. 1999), using alternative choices for distance and reddening

correction. On the basis of linear period relations and evolutionary tracks, either canonical or with a mild convective core overshooting, they concluded that all evolutionary computations predict masses which are systematically larger for a fixed luminosity, especially toward the longest periods. In this context, let us also quote Bono et al. (2002) and Keller & Wood (2002), who studied LMC bump Cepheids and found that the Cepheids are $\sim 15\%$ less massive (or $\sim 20\%$ more luminous) for their luminosity (or mass) predicted by canonical (no overshooting) evolutionary models. Finally, Brocato et al. (2004) investigated a selected sample of short-period Cepheids in the LMC cluster NGC 1866 and showed that, under reasonable assumptions for NGC 1866 reddening and distance modulus, it appears difficult to escape the evidence for pulsation masses smaller than the evolutionary ones, either using canonical or mild convective core overshooting computations.

In this investigation, we shall take advantage of the sample of 34 Galactic Cepheids presented by Storm et al. (2004, hereafter S04) to push forward the B01 result by using accurate $PLC$ relations from updated nonlinear pulsating models, together with evolutionary relations which account for the difference between "static" and "mean" magnitudes of the pulsating stars. Actually, previous theoretical studies for classical Cepheids (Caputo et al. 1999, Paper IV; Caputo et al. 2000, Paper V), RR Lyrae stars (Bono et al. 1995; Marconi et al. 2003), and anomalous Cepheids (Marconi et al. 2004) disclosed that the discrepancy between the mean magnitude, i.e. the time average along the pulsation cycle, and the static magnitude (the value the variable would have in case it were a static star) is not negligible, and increases together with the pulsation amplitude.

We present in §2 the pulsation models which have been used to predict suitable analytical relations connecting the period to the pulsator mass, mean magnitude, and color. In Section 3, the evolutionary constraints are discussed, while §4 deals with mass estimates of the observed sample of Galactic Cepheids. These results are discussed in §5 taking also into account the uncertainties due to Cepheid chemical composition, absolute distance, and reddening. The conclusions of this investigation are briefly outlined in §6.

## 2. Pulsational constraints

During the last few years, we provided theoretical predictions for classical Cepheids as based on a wide grid of nonlinear, nonlocal, and time-dependent convective pulsational models. The first series of computations (Bono et al. 1999b, Paper II) includes the pulsational properties (e.g., period and light curve) of stellar structures, covering a wide range of effective temperatures, stellar masses ranging from 5 to $11 M_{\odot}$, and a solar-like chemical composition (Z=0.02, $Y$=0.28). For each mass, the luminosity level was fixed according to

the mass-luminosity ($ML$) relation predicted by canonical evolutionary tracks by Castellani et al. (1992, hereafter CCS). This theoretical framework also provides the boundaries of the instability strip. In subsequent papers, we presented similar results, but for different masses, luminosities, and helium contents. That set of models has been further implemented with new computations for the present investigation. The assumptions on the input physics and computing procedures have already been presented (see Bono et al. 1999a, Paper I; Bono et al. 2000a, Paper III; Bono et al. 2000c, Paper VI), and will not be discussed here.

The complete set of available fundamental models with Z=0.02 is listed in Table 1[1]. For each given mass, several luminosity levels are explored, thus covering current uncertainties on canonical $ML$ relations (Castellani et al. 1992; Bono et al. 2000b: hereafter B0), as well as accounting for the occurrence of "overluminous" stellar structures as produced by convective core overshooting and/or mass loss. The Period-Luminosity distribution of all the $Z$=0.02 fundamental pulsators is shown in Fig. 1, where solid points display the models computed adopting the B0 canonical $ML$ relation (see Section 3).

Following the procedure discussed in our previous works, the bolometric light curve of the pulsating models was transformed into the observational bands $BVRIJK$ by means of model atmospheres by Castelli et al. (1997a, 1997b), and these light curves are used to derive for each pulsator the magnitude-averaged ($M_i$) and the intensity-averaged $\langle M_i \rangle$ magnitudes over the pulsation cycle. Figure 2[2] shows the ensuing $\langle M_V \rangle$ and $\langle M_K \rangle$ magnitudes as a function of the period. As expected, the intrinsic scatter of the Period-Magnitude distribution, which for any given $ML$ relation is due to the finite width of the instability strip, shows a substantial decrease when passing from visual to near-infrared magnitudes. Concerning the distribution of the fundamental pulsators in the color-magnitude diagram, we show in Fig. 3 the $\langle M_V \rangle$ magnitudes versus the $\langle M_B \rangle - \langle M_V \rangle$ colors.

It is well known that a restatement of the Stefan's law for pulsating variables yields that the pulsation period is uniquely defined by the mass, the luminosity, and the effective temperature of the variable. Once bolometric corrections and color-temperature relations are adopted, this means that the pulsator absolute magnitude $M_i$ in a given photometric bandpass is a function of the pulsator period, stellar mass, and color index $[CI]$, i.e.,

$$\langle M_i \rangle = a + b \log P + c \log M/M_\odot + d[CI] \tag{1}$$

As a matter of fact, a linear interpolation through all the models listed in Table 1 gives,

[1]The Table 1 is only available in the on-line edition of the manuscript.

[2]The figures 2,3, and 11 are only available in the on-line edition of the manuscript.

*independently of any assumption on the ML relation*, tight mass-dependent $PLC$ relations, as shown in the top panel of Fig. 4, for $\langle M_V \rangle$ magnitudes and $\langle M_B \rangle - \langle M_V \rangle$ colors. The entire set of $PLC$ relations is given in Table 2, where the intrinsic dispersion $\sigma_{PLC}$ includes the variation of the helium content from $Y$=0.25 to $Y$=0.31. By using these relations, together with measured absolute magnitudes and intrinsic colors, the pulsation mass $M_p$ of each individual Cepheid can be determined with the intrinsic accuracy $\epsilon_{PLC}(\log M_p)$ given in the last column of the same table. For a Cepheid sample located at the same distance and with the same reddening, one can estimate the mass range covered by the variables, and in turn, the slope of the empirical $M_pL$ relation, independently of the distance and reddening correction. Indeed, the BBK analysis of LMC and SMC Cepheids, which basically adopts a "static" $PLC$ relation, yields mass-luminosity distributions characterized by similar slopes and intrinsic scatters for the three different choices of distance and reddening.

A glance at the results given in Table 2 shows that the coefficients of the color term are not dramatically different from the extinction-to-reddening ratios $A_V/E(B-V)$=3.30, $A_R/E(V-R)$=5.29, $A_I/E(V-I)$=1.52, $A_J/E(V-J)$=0.33, and $A_K/E(V-K)$=0.10 provided by optical and near-infrared reddening models (see, e.g., Caldwell & Coulson 1987; Dean et al. 1978; Laney & Stobie 1993; S04). This is no surprise: as already discussed in several papers (see, e.g., Madore 1982; Madore & Freedman 1991; Tanvir 1999; Caputo et al. 2000), the effect of the interstellar extinction is similar to the intrinsic scatter, due to the finite width of the instability strip. Hence, the adoption of the various reddening insensitive Wesenheit functions ($WBV = V - 3.30(B-V)$, $WVI = I - 1.52(V-I)$, etc.) significantly reduces the dispersion of magnitudes at a given period. This is shown in the bottom panel of Fig. 4, which deals with $\langle WBV \rangle$ functions.

Assuming once again that the $ML$ relation is a free parameter, a linear interpolation through all the fundamental models listed in Table 1 gives the predicted mass-dependent Period-Wesenheit ($PW$) relations listed in Table 3. These relations can be used to estimate the pulsation mass of Cepheids with known distance, independently of reddening. Moreover, if the variables are at the same distance, the mass range can be derived even if a differential reddening is present. However, it is worth noting that a residual effect, due to the finite width of the instability strip, is still present in the $PW$ relations (see the discussion in Madore & Freedman 1991) and, consequently, the intrinsic dispersion $\sigma_{PW}$ [column (4)] is larger than $\sigma_{PLC}$ and the pulsation mass can now be determined with lower accuracy [$\epsilon_{PW}$ in column (5)] than in the case of pulsation masses based on the $PLC$ relations, in particular for $B-V$ colors.

In passing, we note that the edges of the Cepheid instability strip depend both on the $ML$ relation and on the value of the mixing-length parameter $l/H_p$ adopted to close the

system of convective transport and conservation equations. Consequently, these two parameters affect the predicted Period-Luminosity ($PL$) relations, mostly in the visual bands, and play a role in the debated question of the metallicity correction to the Cepheid intrinsic distance modulus, $\mu_0$, derived from the $PL$ relations calibrated on LMC Cepheids (see Paper II and Paper V). Furthermore, Fiorentino et al. (2002, Paper VIII) have shown that *sign and amount* of the predicted correction to LMC-based distances depend on both the helium and metal content of the variable, mainly for Cepheids with $Z > 0.008$. In our previous papers, we showed that the theoretical results, based on canonical $ML$ relations and $l/H_p$=1.5, supply a viable approach for reducing the apparent discrepancy between the Cepheid and the maser distance to the galaxy NGC 4258 (Caputo et al. 2002). The same predictions can also account for the empirical metallicity correction $\delta\mu_0/\delta\log Z \sim$+0.24 mag dex$^{-1}$ derived by Kennicutt et al. (1998), using Cepheids in two fields of the galaxy M101, provided that a helium-to-metal enrichment ratio $\Delta Y/\Delta Z \sim 3.5$ is adopted. Moreover, recent high resolution, high signal-to-noise spectra for three dozen of Galactic and Magellanic Cepheids (Mottini et al. 2004; Romaniello et al. 2004), and absolute distances based on the near-infrared surface brightness method (S04) support the quoted theoretical framework. Even though current pulsation models appear to be validated by empirical evidence, it is worth underlining that both $PLC$ and $PW$ relations, at variance with the $PL$ relation, are practically unaffected by the adopted $l/H_p$ value. Moreover, the inclusion into these relations of the mass dependence overcomes the assumption on the $ML$ relation.

Finally, we take into account metal contents slightly different than $Z$=0.02, as suggested by individual abundance determinations for Galactic Cepheids (see e.g., Fry & Carney 1997; Andriewsky et al. 2002a,b,c; Luck et al. 2003; Romaniello et al. 2004). According to fundamental models constructed by adopting $Z$=0.03 (Paper VIII) and $Z$=0.01 (Marconi et al. 2004, in preparation), we estimated the metallicity effect on the predicted $PLC$ and $PW$ relations. We find that the corrections on the estimated mass for $BV$ and $VR$ colors are: $\Delta\log M_p \sim -0.35(\pm0.03)\log(Z/0.02)$ and $\sim -0.23(\pm0.02)\log(Z/0.02)$, while for $VI$, $VJ$, and $VK$ colors are: $\Delta\log M_p \sim +0.02(\pm0.02)\log(Z/0.02)$. The latter values indicate that there is no significant variation, at least in the range $Z$=0.01 to 0.03.

## 3. Evolutionary constraints

The main evolutionary properties of central He-burning intermediate-mass stars have been extensively discussed in several papers (see, e.g., Girardi et al. 2000, hereafter G00; B01; Castellani et al. 2003, and references therein), and we wish only to mention that, for fixed chemical composition and physical assumptions, the crossing of the Cepheid instability strip

occurs with a characteristic "blue loop", whose luminosity is almost uniquely determined by the original stellar mass. bf The reader interested in a detailed discussion concerning the dependence of the blue loop on input physics and physical assumptions is referred to Chiosi, Bertelli, & Bressan (1992), Stothers & Chin (1994), and Cassisi (2004), and references therein. On this ground, the relevant literature contains several theoretical $ML$ relations, which are widely used to estimate the Cepheid evolutionary mass.

In this investigation, using the B0 canonical evolutionary models, which are computed with the same physics of the pulsating models, we adopt for the canonical $ML$ relation in the mass range 4-15$M_{\odot}$ the following relation:

$$\log(L/L_{\odot})_{can} = 0.72 + 3.35 \log M/M_{\odot} + 1.36 \log(Y/0.28) - 0.34 \log(Z/0.02) \qquad (2)$$

with a standard deviation $\sigma$=0.04, which accounts for both the blueward and the redward portion of the blue loop ($2^{nd}$ and $3^{rd}$ crossing of the Cepheid instability strip).

The introduction of a $ML$ relation, which connects the permitted values of mass and luminosity, gives a two-parameter description of the pulsator luminosity. Typically, as originally suggested in the pioneering investigations by Sandage (1958), Sandage & Gratton (1963), and by Sandage & Tammann (1968), the mass-term of equation (1), if we account for evolutionary constraints, can be removed in order to have a $PLC$ relation. However, since our purpose is to determine the pulsation mass, from a linear interpolation through all the fundamental models listed in Table 1, we derive the predicted Mass-Period-Luminosity ($MPL$) and the Mass-Color-Luminosity ($MCL$) relations given in Table 4 and in Table 5, respectively. These relations, which are valid for structures with $Z$=0.02, $Y$=0.28$\pm$0.03, account for the quoted uncertainty of $\sigma$=0.04 in the B0 canonical $ML$ relation, and are based on intensity-averaged magnitudes. Moreover, they include the effects of evolutionary $ML$ relations different from equation (2). Therefore, once the $L/L_{can}$ ratio is specified, where $L_{can}$ is given by equation (2), these relations can be used to estimate the evolutionary mass of Cepheids at its best with an intrinsic accuracy $\epsilon(\log M_e) \sim 0.03$ (see last column in Table 4 and in Table 5).

In the end of this section, two points are worth noticing:

1. by using the entire set of fundamental models with metal content in the range $Z$=0.01-0.03, we find that the evolutionary mass inferred by the predicted $MPL$ and $MCL$ relations in Table 4 and Table 5, respectively, varies as $\Delta \log M_e \sim 0.01 \log(Z/0.02)$, for fixed $L/L_{can}$ ratio;

2. at fixed chemical composition, any change in luminosity relative to the canonical value $L_{can}$ leads to a variation in the estimated evolutionary masses. Therefore, the occurrence of overluminous stellar structures produced by convective core overshooting ($\log L/L_{can} \sim 0.20$ at fixed mass, see Chiosi et al. 1993) yields evolutionary masses smaller than the canonical values. By using $MPL$ relations, we obtain $\Delta \log M_e \sim -0.03$ ($K$ magnitudes) to $\sim -0.06$ ($V$ magnitudes), while with $MCL$ relations it is $\Delta \log M_e \sim -0.06$ independently of the adopted color.

## 4. Masses of Galactic Cepheids

The recent paper by S04 gives $BVIJK$ absolute magnitudes of 34 Cepheids in the Milky Way with solar-like metal content ([Fe/H]=0.03±0.14). This means that we can determine the pulsation mass from the predicted $PLC$ relations (see Table 2) and the evolutionary one from the $MPL$ or the $MCL$ relations (see Table 4 and Table 5). For the sake of the following discussion, let us first summarize in Table 6 a global estimate of the uncertainties affecting the mass determinations as due to $ML$ relations different from equation (2) as well as to variations of the Cepheid intrinsic properties (period and metal content) and observational parameters (distance and reddening).

Starting with the $PLC$ relations, we give in Table 7 the pulsation mass determination [column (4) and columns (6) to (8)] together with the associated error [column (5) and column (9)] as determined by the intrinsic uncertainty of the $PLC$ relations [column (5) in Table 2] and the error on the Cepheid intrinsic distance modulus (see S04). As also shown in Fig. 5, where open dots refer to the short-period variables SU Cas and EV Sct, the various estimates are in reasonable agreement with each other, but with some evidence of the mass value increasing, on average, when passing from $BV$ to $VK$ colors. In this context, it should be mentioned that the reddening values adopted by S04 came from different sources, and that any uncertainty on this parameter affects the $BV$-based pulsation mass estimates in the opposite way when compared with $VI$, $VJ$, and $VK$ colors (see Table 6). Moreover, we note that by adopting for the Galactic Cepheids the new metallicity $Z \sim 0.01$ recently suggested for the Sun (Asplund et al. 2004) we find that the $BV$-based pulsation masses should be increased by $\Delta \log M_p \sim 0.11$, but marginally affects the other estimates. Therefore, we decide to adopt for the following discussion the average value $\langle \log M_p \rangle$ of the $VIJK$-based mass estimates together with a final error, which includes both the value listed in column (9) of Table 7 and the standard error on the mean.

We now use the predicted $MPL$ relations given in Table 4 to estimate the canonical ($L = L_{can}$) evolutionary masses at $Z$=0.02 and $Y$=0.28±0.03. The results are listed in Table

8 [columns (4) to (7)] together with the average associated error [column (8)] as determined by the intrinsic uncertainty of the $MPL$ relations and the error on the Cepheid distance. Data plotted in Fig. 6 show that there is now a better agreement among the various estimates, even though the estimated mass slightly decreases when moving from visual to near-infrared magnitudes. In particular, $K$-magnitudes would lead to masses smaller by $\Delta \log M_e \sim 0.05$ than visual magnitudes. A glance at the data listed in Table 6 suggests that the effects of distance and reddening on the evolutionary masses based on the predicted $MPL$ relations are $\Delta \log M_e(V) \sim 0.11\Delta\mu_0 + 0.36\Delta E(B-V)$ and $\Delta \log M_e(K) \sim 0.26\Delta\mu_0 + 0.08\Delta E(B-V)$. Therefore, the results plotted in the bottom panel of Fig. 6 might suggest that, on average, the adopted distances should be increased by $\sim 0.3$ mag (for fixed reddening), or the adopted reddening decreased by $\sim -0.2$ mag (for fixed distance), or a combination of the two effects. Alternatively, a breakdown of the canonical $ML$ relation should be considered (see point 2 in the previous section and Table 6), with the condition $M_e(V)=M_e(K)$ requiring for each given mass a luminosity increased by $\Delta \log L \sim 0.25$ with respect to the canonical level, as predicted by convective core overshooting evolutionary models.

Concerning the evolutionary mass inferred by the $MCL$ relations, the results are listed in Table 9 [columns (4) to (7)] together with the average associated error [column (8)]. As shown in Fig. 7, the agreement among the various determinations is now extremely good as a consequence of the fact that uncertainties on the adopted $ML$ relation or on the Cepheid parameters (metal content, distance, and reddening) affect the results by almost the same quantity, independently of the adopted color (see Table 6). On this ground, we adopt for the following discussion the average $\langle \log M_{e,can} \rangle$ of the $MCL$-based mass estimates with a final error which includes both the value in column (8) of Table 9 and the standard error on the mean.

## 5. Discussion

The pulsation and evolutionary masses -$\langle \log M_p \rangle$, $\langle \log M_{e,can} \rangle$- estimated in §4, are presented in Fig. 8. We find that the entire Cepheid sample shows $M_{e,can} \geq M_p$. There are three exceptions: SU Cas and EV Sct (open dots) and the long-period variable l Car. Moreover, data plotted in this figure show that the discrepancy between the pulsation and the evolutionary mass increases when moving from high to low-mass Cepheids.

Let us briefly discuss the two short-period variables (SU Cas, EV Sct) with $M_p > M_{e,can}$. By using the derivatives given in Table 5, we note that a variation in the pulsation period only affects the pulsation mass as $\Delta \langle \log M_p \rangle \sim -1.13\Delta \log P$. Consequently, if SU Cas and EV Sct are first overtone (FO) pulsators and their period is fundamentalised as $\log P_F \sim$

$\log P_{FO}$+0.14, then the pulsation mass decreases by $\Delta \log M_p \sim 0.16$, thus leading them to follow the behavior of the other variables. This would confirm early suggestions that SU Cas (see, e.g., Gieren 1982; Evans 1991; Fernie et al. 1995; Andrievsky et al. 2002c) and EV Sct (Tammann et al. 2003; Groenewegen et al. 2004) might be FO pulsators. However, these two objects need to be handled with care, since SU Cas is connected with a reflection nebula (van den Bergh 1966) and EV Sct appears to show an unusual line profile structure (Kovtyukh et al. 2003).

For the remaining Cepheids which are, according to Fernie et al. (1995), fundamental pulsators, we plot in the top panel of Fig. 9 the ratio $M_p/M_{e,can}$ as a function of the pulsation period. Note that, in order to minimize the effects of uncertainties on the adopted reddening (see Table 6), we consider only the pulsation and evolutionary mass estimates based on $PLC(VK)$ and $MCL(VK)$ relations, respectively. Current results suggest that the $M_p/M_{e,can}$ ratio decreases from long-period to short-period variables, thus supporting earlier suggestions by B01 and Gieren (1989). Data plotted in the bottom panel of the same figure show that the inclusion of mild convective core overshooting (i.e., by adopting $\log L/L_{can}$=0.2) does not affect the pulsation masses, but yields systematically smaller evolutionary masses, with the unfortunate consequence of several variables showing $M_p > M_{e,over}$. By the way, this result allows us to drop the hypothesis of noncanonical luminosity levels, so as to solve the mild discrepancy between $M_{e,can}(V)$ and $M_{e,can}(K)$ values discussed in Section 3.

In order to test the dependence of current findings on the adopted $ML$ relation, we also adopted the $ML$ relation provided by G00 and based on canonical evolutionary computations with $Z$=0.019, $Y$=0.273, and stellar masses in the range 4-8$M_\odot$. The top panel of Fig. 10 shows the comparison between the average luminosity predicted by G00 for canonical central He-burning models (solid line) and the luminosity given by equation (2) (dashed line). The two sets of models present different slopes of the $ML$ relation (see also Fig. 5 in BBK), in particular the G00 models appear fainter for stellar masses $< 5M_\odot$ and brighter for masses $> 5M_\odot$ than predictions based on B0 computations. As a consequence, (see the bottom panel in the same figure) the adoption of the G00 canonical models leads to a steeper dependence of the $M_p/M_{e,can}$ ratio on the Cepheid period, and to an increased number of variables with $M_p > M_{e,can}$. The inclusion of mild convective core overshooting makes the situation even worse: owing to the increased luminosity for any fixed mass, all the $M_p/M_e$ ratios become systematically larger and almost all the Cepheids would have evolutionary masses smaller than the pulsation ones.

The discussion of the evolutionary models is beyond the purpose of the present paper; however, the results presented in Fig. 9 and Fig. 10 show that the current evolutionary

scenario is affected not only by the assumptions on the efficiency of overshooting, but also by sizable differences (e.g., the equation of state) in the canonical models. Here, relying on the S04 distance determinations, we feel that the canonical B0 computations offer the most palatable evolutionary scenario for studying the relation between the Cepheid pulsation mass and the evolutionary one, *under the assumption of no mass-loss*. Therefore, the trend of the $M_p/M_{e,can}$ ratio with the Cepheid period disclosed in the top panel of Fig. 9 should be considered as real, unless there are significant faults with our approach or significant errors in the Cepheid adopted distance and reddening. In order to remove any doubt on the reliability of the adopted procedure, we use all the pulsation models listed in Table 1 as real Cepheids, and we derive their mass from the predicted $PLC$ and $MCL$ relations. We show in Fig. 11 that the ensuing ratio between the pulsation and the evolutionary mass is $M_p/M_{e,can}$=1$\pm$0.05, which is a quite irrelevant uncertainty with respect to the results in Fig. 9. On the other hand, according to the derivative values listed in Table 6, the condition log$M_p(VK)$=log$M_{e,can}(VK)$ for the observed Cepheids would imply rather unrealistic corrections to the adopted distance and reddening value as given, e.g., by $\Delta\mu_0 \sim 0.5$ mag or $\Delta E(B-V) \sim -0.4$ mag at log$P$=0.6.

To further constrain the plausibility of current theoretical predictions we decided to perform a comparison with the dynamical mass of S Mus. This object is the binary Cepheid with the hottest known companion and Evans et al. (2004) by using spectra collected with both the Hubble Space Telescope and the Far Ultraviolet Spectroscopic Explorer estimated a mass of $M = 6.0 \pm 0.4 M_{\odot}$.This mass determination agrees quite well with the estimates of similar binary Cepheids (Böhm-Vitense et al. 1997), but presents a smaller uncertainty. By adopting for S Mus the following input parameters: P=9.6599 days, $V$=6.118 (Fernie et al. 1995), E$(B-V)$=0.23 (Evans et al. 2004), $K$=3.987 (Kimeswenger et al. 2004), and by using the $K$-band PL relation provided by S04, we found a true distance modulus of $\mu_0 = 9.55 \pm 0.15$ mag. By using these data and the PW $(V-K)$ relation (see Table 3) we find for S Mus a pulsation mass of $M = 5.6 \pm 0.8 M_{\odot}$, while by assuming $L = L_{can}$ and the MPL $(M_K)$ relation (see Table 4) we find an evolutionary mass of $6.3 \pm 0.6 M_{\odot}$. According to Fernie et al. (1995) the reddening of S Mus is E$(B-V)$=0.15, and in turn, the true distance modulus becomes $\mu_0 = 9.58 \pm 0.15$. Stellar masses based on these values are only marginally different, i.e. $M = 5.8 \pm 0.8 M_{\odot}$ (PW), $6.3 \pm 0.6 M_{\odot}$ (MPL). Note that the uncertainties affecting current mass estimates account for both the error on the distance modulus and for the intrinsic dispersion of evolutionary and pulsation relation. Pulsation and evolutionary mass agree, within the errors with the dynamical mass. However, no firm conclusion can be reached concerning the mass discrepancy, due to current empirical and theoretical uncertainties. An independent mass estimate for S Mus was recently provided by Petterson, Cottrell, & Albrow (2004), by using high resolution spectroscopy they found

$M = 6.2 \pm 0.2 M_{\odot}$. It is noteworthy, that dynamical mass of binary Cepheids might play a crucial role in settling the discrepancy between evolutionary and pulsation masses, since these determinations give the actual Cepheid masses.

In conclusion, since the pulsation mass is the actual mass of the Cepheids, whereas the evolutionary one is based on canonical evolutionary models neglecting mass-loss, we are quite confident that the estimated $M_p/M_{e,can}$ ratios plotted in the top panel of Fig. 9 reflect a mass-loss occurring during or before the central He-burning phase. Figure 12 shows the ensuing ratio between the difference $\Delta M = M_{e,can} - M_p$ and the canonical evolutionary mass as a function of $M_{e,can}$. Taken at face value, the data give sufficiently firm evidence for a mass-loss efficiency, which decreases where increasing the Cepheid original mass. The discrepancy ranges from $\sim 20\%$ at $4M_{\odot}$ to $\sim 0$ around $13M_{\odot}$. This finding might appear at variance with empirical evidence, since current semi-empirical stellar wind parametrizations indicate that the mass-loss rate in early and in late type stars is correlated with both stellar luminosity and radius (Reimers 1975; Nieuwenhuijzen & de Jager 1990). However, current evolutionary models predict that central He-burning phases are significantly longer when moving from higher to lower intermediate-mass stars. In particular, the central He lifetime at solar chemical composition (Y=0.27, Z=0.02) increases from $\sim 2$ Myr for stellar structures with $M = 12M_{\odot}$ to $\sim 22$ Myr for $M = 5M_{\odot}$. Moreover and even more importantly, the blue loop of the latter structure attains cooler effective temperatures when compared with the former one. The hottest effective temperature reached by the two structures along the blue loop increases from $\sim 6000$ K for $M = 5M_{\odot}$ to 14,000 K for $M = 12M_{\odot}$ (see, e.g. Table 3 and Fig. 3 in B0). These intrinsic properties provide a plausible explanation for the increased mass loss efficiency among short-period Cepheids. Finally, we notice that the peculiar result $M_p/M_{e,can}$=1.14 for the long-period variable l Car might suggest that this Cepheid is on its first crossing of the instability strip. In this case, a decrease in the luminosity of $\Delta \log L \sim -0.2$, with respect to the $2^{nd}$ and $3^{rd}$ crossing luminosity, would imply $M_p \approx M_e$.

## 6. Conclusions

The comparison between theory and observations indicates that the discrepancy between pulsation and evolutionary mass might be due to mass-loss. However, this finding relies, as suggested by the referee, on the accuracy of Baade-Wesselink (BW) distance determinations. A possible luminosity dependent error cannot be excluded. In particular, angular diameters and linear variations present a discrepancy in the phase interval between 0.8 and 1.0 (see Fig. 2 in S04). In order to overcome this problem, it has been suggested by Sabbey et al. (1995)

that the conversion factor between radial and pulsation velocity, the so-called $p$-factor, is not constant along the pulsation cycle as assumed in the BW method and its variants (Barnes & Evans 1976). However, recent time-dependent models for $\delta$ Cep by Nardetto et al. (2004) suggest that the time dependence of the $p$-factor is marginal. Moreover and even more importantly, we still lack firm theoretical and empirical constraints on the dependence of the $p$-factor on the pulsation period (Gieren et al. 1993; Marengo et al. 2004, and references therein).

The occurrence of mass-loss was theoretically predicted by Iben (1974) in his seminal investigation of the evolution of intermediate-mass stars. Indeed, the computations by this author did not exclude the possibility that these stars loose almost one third of their original mass during the giant phase. Moreover, as suggested by Wilson & Bowen (1984), stellar pulsation may play a key role in causing or at least enhancing mass-loss. In his comprehensive review, Cox (1980) discussed the discrepancies he found by using different approaches to obtain Cepheid masses. In particular, the pulsation masses seemed to agree within the error with the evolutionary ones available at that time, but the intrinsic scatter of the ratio between the two estimates was quite large, namely $M_p/M_e = 0.97 \pm 0.25$ for homogeneous models and 1.07±0.27 for unhomogeneous models. Gieren (1982), on the basis of a new analysis of different methods to derive Cepheid masses, found smaller scatters around the above ratio, but a discrepancy between pulsation and evolutionary masses (with the former smaller than the latter), which increases toward longer periods.

On the observational side (see Szabados 2003 for a review and references), evidence of mass-loss during or prior the Cepheid phase is still a rather elusive issue. Empirical estimates based on infrared and ultraviolet emissions and VLA observations would suggest mass-loss rates from $10^{-10}$ to $10^{-7} M_{\odot}\mathrm{yr}^{-1}$. It is also questionable whether the mass-loss efficiency is independent of the pulsation period or not. As an example, IRAS data suggest roughly constant values, whereas IUE spectra indicate that the mass-loss rate in $\zeta$ Gem ($\log P$=1.007) is 3 times smaller than the value of l Car ($\log P$=1.551). However, together with the mass-loss rate, one should also account for the He-burning evolutionary times, which significantly increase when decreasing the original Cepheid mass (i.e. from long to short-period variables).

In conclusion, current empirical estimates concerning the efficiency of mass-loss in classical Cepheids are limited to a few objects and probably affected by systematic uncertainties (Deasy 1988; Szabados 2003). Moreover, it is not clear whether binarity might enhance the mass-loss rate. Therefore, the pulsational properties appear as a robust approach to get information on mass-loss in classical Cepheids. In this context, the pulsation masses might also provide fundamental constraints upon future evolutionary model computations.

It is a pleasure to thank V. Castellani for several comments and suggestions on an early draft of this paper. We also wish to acknowledge an anonymous referee for his/her positive comments and pertinent suggestions that helped us to improve the content and the readability of the manuscript. Financial support for this study was provided by PRIN 2002,2003 within the framework of the projects: "Stellar populations in the Local Group" (P.I.: M. Tosi) and ''Continuity and Discontinuity in the Milky Way Formation" (P.I.: R. Gratton). This project made use of computational resources granted by the "Consorzio di Ricerca del Gran Sasso" according to the "Progetto 6: Calcolo Evoluto e sue applicazioni (RSV6) - Cluster C11/B".

## REFERENCES

Andrievsky, S. M., Bersier, D., Kovtyukh, V. V., Luck, R. E., Maciel, W. J., Lepine, J. R. D., Beletsky, & Yu. V. 2002a, A&A, 384, 140

Andrievsky, S. M., Kovtyukh, V. V., Luck, R. E., Lepine, J. R. D., Maciel, W. J., & Beletsky, Yu. V. 2002b, A&A, 392, 491

Andrievsky, S. M., et al. 2002c, A&A, 381, 32

Asplund, M., Grevesse, N., Sauval, A. J., Allende Prieto, C., & Kiselman, D. 2004, A&A, 417, 751

Barnes, T., & Evans, D. 1976, MNRAS, 174, 489

Beaulieu, J. P., Buchler, J. R., & Kollath, Z. 2001, A&A, 373, 164 (BBK)

Bohm-Vitense, E., Evans, N. R., Carpenter, K., Morgan, S., Beck-Winchatz, B., & Robinson, R. 1997, AJ, 114, 1176

Bono, G., Caputo, F., Cassisi, S., Marconi, M., Piersanti, L., & Tornambé, A. 2000b, ApJ, 543, 955 (B0)

Bono, G., Caputo, F., & Stellingwerf, R. F. 1995, ApJS, 99, 263

Bono, G., Caputo, F., Castellani, V., & Marconi, M. 1999b, ApJ, 512, 711 (Paper II)

Bono, G., Castellani, V., & Marconi, M. 2000a, ApJ, 529, 293 (Paper III)

Bono, G., Castellani, V., & Marconi, M. 2002, ApJ, 565, 83

Bono, G., Gieren, W. P., Marconi, M., Fouqu, P., & Caputo, F. 2001, ApJ, 563, 319 (B01)

Bono, G., Marconi, M., & Stellingwerf, R. F. 1999a, ApJS, 122, 167 (Paper I)

Bono, G., Marconi, M., & Stellingwerf, R. F. 2000c, A&A, 360, 245 (Paper VI)

Brocato, E., Caputo, F., Castellani, V., Marconi, M., Musella, I., 2004, AJ, 128, 1597

Caldwell, J. A. R., & Coulson, I. M. 1987, AJ, 93, 1090

Caputo, F., Marconi, M., & Musella, I. 2000, A&A, 354, 610 (Paper V)

Caputo, F., Marconi, M., & Musella, I. 2002, ApJ, 566, 833

Caputo, F., Marconi, M., & Ripepi, V. 1999, ApJ, 525, 784 (Paper IV)

Cassisi, S. 2004, in IAU Colloq. 193, Variable Stars in the Local Group, ed. D.W. Kurtz & K.R. Pollard. (San Francisco: ASP), 489

Castellani, V., Chieffi, A., & Straniero, O. 1992, ApJS, 78, 517 (CCS)

Castellani, V., Degl'Innocenti, S., Marconi, M., Prada Moroni, P. G., & Sestito, P. 2003, A&A, 404, 645

Castelli, F., Gratton, R. G., & Kurucz, R. L. 1997a, A&A, 318, 841

Castelli, F., Gratton, R. G., & Kurucz, R. L. 1997b, A&A, 324, 432

Chiosi, C., Bertelli, G., & Bressan, A. 1992, ARAA, 30, 235

Chiosi, C., Wood, P. R., & Capitanio, N. 1993, ApJS, 86, 541

Cox, A. N. 1980, ARA&A, 18, 15

Dean, J. F., Warren, P. R., & Cousins, A. W. J. 1978, MNRAS, 183, 569

Deasy, H. P. 1988, MNRAS, 231, 673

Evans, N. R. 1991, ApJ, 372, 597

Evans, N. R., Massa, D., Fullerton, A., Sonneborn, G., Iping, R. 2004, in IAU Colloq. 193, Variable Stars in the Local Group, ed. D.W. Kurtz & K.R. Pollard (San Francisco: ASP), 377

Fernie, J. D., Evans, N. R., Beattie, B., & Seager, S. 1995, IBVS, 4148, 1

Ferrarese, L. et al. 2000, ApJS, 128, 431

Fiorentino, G., Caputo, F., Marconi, M., & Musella, I. 2002, ApJ, 576, 402 (Paper VIII)

Freedman, W. L., HST Key Project 2001, ApJ, 553, 47

Fry, A. M., & Carney, B. W. 1997, AJ, 113, 1073

Gieren, W. 1982, ApJ, 260, 208

Gieren, W. 1989, A&A, 225, 381

Gieren, W. P., Barnes, T. G., & Moffett, T. J. 1993, ApJ, 418, 135

Girardi, L., Bressan, A., Bertelli, G., & Chiosi, C. 2000, A&AS, 141, 371 (G00)

Groenewegen, M. A. T., Romaniello, M., Primas, F., & Mottini, M. 2004, A&A, 420, 655

Iben, I., Jr. 1974, ARA&A, 12, 215

Keller, S.C., & Wood, P.R. 2002, ApJ, 578, 144

Kennicutt, R. C. et al. 1998, ApJ, 498, 181

Kimeswenger, S., et al. 2004, A&A, 413, 1037

Kovtyukh, V. V., Andrievsky, S. M., Luck, R. E., Gorlova, N. I. 2003, A&A, 401, 661

Laney, C. D. & Stobie, R. S. 1993, MNRAS, 263, 921

Luck, R. E., Gieren, W. P., Andrievsky, S. M., Kovtyukh, V. V., Fouqué, P., Pont, F., & Kienzle, F. 2003, A&A, 401, 939

Madore, B. F. 1982, ApJ, 253, 575

Madore, B. F., & Freedman, W. L. 1991, PASP, 103, 933

Marengo, M., Karovska, M., Sasselov, D. D., & Sanchez, M. 2004, ApJ, 603, 285

Marconi, M., Caputo, F., Di Criscienzo, M., & Castellani, M. 2003, ApJ, 596, 299

Marconi, M., Fiorentino, G., & Caputo, F. 2004, A&A, 417, 1101

Mottini, M., Romaniello, M., Primas, F., Groenewegen, M., Bono, G., & Francois P. 2004, astro-ph/0411190

Nardetto, N., Fokin, A., Mourard, D., Mathias, Ph., Kervella, P., & Bersier, D. 2004, A&A, 428, 131

Nieuwenhuijzen, H., & de Jager, C. 1990, A&A, 231, 134

Petterson, O. K. L., Cottrell, P. L., Albrow, M. D. 2004, MNRAS, 350, 95

Reimers, D. 1975, Mém. Soc. Roy. Sci. Liége $6^e$ Ser., 8, 369

Romaniello, M., Primas, F., Mottini, M., Groenewegen, M., Bono, G., & Francois, P. 2004, A&A, 429, L37

Sabbey, C. N., Sasselov, D. D., Fieldus, M. S., Lester, J. B., Venn, K. A., & Butler, R. P. 1995, ApJ, 446, 250

Saha, A. et al. 2001, ApJ, 562, 314

Sandage, A. 1958, ApJ, 127, 513

Sandage, A., & Gratton, L. 1963, in Star Evolution, XXVIIIth Course of the International School of Physics "Enrico Fermi", ed. L. Gratton, (New York: Academic Press), 11

Sandage, A., & Tammann, G. A. 1968, ApJ, 151, 531

Storm, J., Carney, B. W., Gieren, W. P., Fouqué, P., Latham, D. W., & Fry, A. M. 2004, A&A, 415, 531 (S04)

Stothers, R. B., & Chin, C. W. 1994, ApJ, 431, 797

Szabados, L. 2003, CoKon, 103, 115

Tammann, G. A., Sandage, A., & Reindl, B. 2003, A&A, 404, 423

Tanvir, N. R., 1999, in Post-Hipparcos cosmic candles, ed. A. Heck & F. Caputo, (Boston: Kluwer Academic Publishers), 17

Udalski, A., Soszynski, I., Szymanski, M., Kubiak, M., Pietrzynski, G., Wozniak, P., &, Zebrun, K. 1999, AcA, 49, 223

van den Bergh, S. 1966, AJ, 71, 990

Wilson, L. A., & Bowen, G. H. 1984, Nature, 312, 429

This preprint was prepared with the AAS LaTeX macros v5.2.

Table 1: Intrinsic parameters for $Z$=0.02 fundamental pulsators.

| $Y$ | $M/M_{\odot}$ | log$L/L_{\odot}$ | $ML$ | Reference |
|---|---|---|---|---|
| 0.25 | 5.00 | 3.000 | B0 | This paper |
| | 7.00 | 3.490 | ” | ” |
| | 9.00 | 3.860 | ” | ” |
| | 11.00 | 4.150 | ” | ” |
| 0.26 | 5.00 | 3.024 | 00 | This paper |
| | 7.00 | 3.512 | ” | ” |
| | 9.00 | 3.878 | ” | ” |
| | 11.00 | 4.171 | ” | ” |
| 0.28 | 4.00 | 2.970 | overl. | B01 |
| | 4.50 | 2.900 | CCS | ” |
| | 5.00 | 3.070 | CCS | B99b |
| | 5.00 | 3.300 | overl. | ” |
| | 6.25 | 3.420 | CCS | B01 |
| | 6.50 | 3.480 | ” | ” |
| | 6.75 | 3.540 | ” | ” |
| | 7.00 | 3.650 | ” | B99b |
| | 7.00 | 3.85 | overl. | ” |
| | 9.00 | 4.000 | CCS | ” |
| | 9.00 | 4.250 | overl. | ” |
| | 11.00 | 4.400 | CCS | ” |
| | 11.00 | 4.650 | overl. | ” |
| 0.31 | 5.00 | 3.130 | B0 | F02 |
| | 7.00 | 3.620 | ” | ” |
| | 9.00 | 3.980 | ” | ” |
| | 11.00 | 4.270 | ” | ” |

Reference: Bono et al. 1999b (B99b); Bono et al. 2000 (B0); Bono et al. 2001 (B01); Castellani et al 1992 (CCS); Fiorentino et al. 2002 (F02).

Table 2: Predicted mass-dependent $PLC$ relations for fundamental pulsators with fixed metal content, $Z$=0.02, and helium abundance ranging from $Y$=0.25 to 0.31, based on intensity-averaged magnitudes of the pulsators. The last two columns give the intrinsic dispersion $\sigma_{PLC}$ of the relation and the intrinsic uncertainty $\epsilon_{PLC}(\log M_p)$ on the pulsation mass inferred by these relations.

| $a$ | $b$ | $c$ | $d$ | $\sigma_{PLC}$(mag) | $\epsilon_{PLC}(\log M_p)$ |
|---|---|---|---|---|---|
| | | $\langle M_V\rangle$=$a$+$b$log$P$+$c$log$M/M_\odot$ +$d$[$\langle B\rangle - \langle V\rangle$] | | | |
| −1.583±0.062 | −2.800±0.045 | −2.103±0.099 | +2.540 ±0.054 | 0.062 | 0.030 |
| | | $\langle M_R\rangle$=$a$+$b$log$P$+$c$log$M/M_\odot$ +$d$[$\langle V\rangle - \langle R\rangle$] | | | |
| −1.903±0.042 | −2.733±0.030 | −2.213±0.066 | +4.739 ±0.081 | 0.042 | 0.020 |
| | | $\langle M_I\rangle$=$a$+$b$log$P$+$c$log$M/M_\odot$+$d$[$\langle V\rangle - \langle I\rangle$] | | | |
| −2.057±0.041 | −2.698±0.028 | −2.266±0.064 | +2.142±0.043 | 0.041 | 0.018 |
| | | $\langle M_J\rangle$=$a$+$b$log$P$+$c$log$M/M_\odot$+$d$[$\langle V\rangle - \langle J\rangle$] | | | |
| −1.707±0.038 | −2.680±0.026 | −2.356±0.059 | +0.707±0.022 | 0.038 | 0.016 |
| | | $\langle M_K\rangle$=$a$+$b$log$P$+$c$log$M/M_\odot$+$d$[$\langle V\rangle - \langle K\rangle$] | | | |
| −1.605±0.040 | −2.626±0.026 | −2.448±0.061 | +0.231±0.016 | 0.040 | 0.016 |

Table 3: Predicted mass-dependent $PW$ relations for fundamental pulsators with $Z$=0.02 and $Y$=0.25 to 0.31, based on intensity-averaged magnitudes of the pulsators. The last two columns give the intrinsic dispersion $\sigma_{PW}$ of the relations and the intrinsic uncertainty $\epsilon_{PW}(\log M_p)$ on the pulsation mass inferred by these relations.

| $a$ | $b$ | $c$ | $\sigma_{PW}$(mag) | $\epsilon_{PW}(\log M_p)$ |
|---|---|---|---|---|
| $\langle M_V\rangle - 3.30[\langle B\rangle - \langle V\rangle] = a + b\log P + c\log M/M_\odot$ | | | | |
| $-2.234\pm0.091$ | $-3.323\pm0.038$ | $-1.491\pm0.129$ | 0.095 | 0.065 |
| $\langle M_R\rangle - 5.29[\langle V\rangle - \langle R\rangle] = a + b\log P + c\log M/M_\odot$ | | | | |
| $-1.708\pm0.066$ | $-2.601\pm0.010$ | $-2.364\pm0.066$ | 0.046 | 0.028 |
| $\langle M_I\rangle - 1.52[\langle V\rangle - \langle I\rangle] = a + b\log P + c\log M/M_\odot$ | | | | |
| $-1.532\pm0.060$ | $-2.371\pm0.025$ | $-2.638\pm0.086$ | 0.060 | 0.025 |
| $\langle M_J\rangle - 0.33[\langle V\rangle - \langle J\rangle] = a + b\log P + c\log M/M_\odot$ | | | | |
| $-1.198\pm0.063$ | $-2.320\pm0.026$ | $-2.751\pm0.089$ | 0.063 | 0.023 |
| $\langle M_K\rangle - 0.10[\langle V\rangle - \langle K\rangle] = a + b\log P + c\log M/M_\odot$ | | | | |
| $-1.372\pm0.059$ | $-2.459\pm0.020$ | $-2.628\pm0.067$ | 0.047 | 0.022 |

Table 4: Predicted intensity-averaged $MPL$ relations for He-burning fundamental pulsators with $Z$=0.02 and $Y$=0.25 to $Y$=0.31. The last column gives the intrinsic uncertainty $\epsilon_{MPL}(\log M_e)$ on the evolutionary mass inferred by these relations due to the above helium content variation and to the intrinsic dispersion, $\sigma$=0.04, in the adopted $ML$ relation. Note that $L_{can}$ is the luminosity of a given mass according to the B0 canonical evolutionary tracks (see text).

| $\langle M_i \rangle$ | $a$ | $b$ | $c$ | $d$ | $\epsilon_{MPL}(\log M_e)$ |
|---|---|---|---|---|---|
| | | $\langle M_i \rangle = a + b\log P + c\log M/M_\odot + d\log(L/L_{can})$ | | | |
| $\langle M_V \rangle$ | +3.24±0.15 | +0.64±0.12 | −9.22±0.31 | −2.99±0.09 | 0.03 |
| $\langle M_R \rangle$ | +2.36±0.12 | +0.06±0.10 | −8.04±0.29 | −2.49±0.08 | 0.03 |
| $\langle M_I \rangle$ | +1.59±0.10 | −0.40±0.08 | −7.07±0.26 | −2.08±0.06 | 0.03 |
| $\langle M_J \rangle$ | +0.40±0.06 | −1.27±0.05 | −5.32±0.16 | −1.31±0.04 | 0.02 |
| $\langle M_K \rangle$ | -0.60±0.04 | −1.95±0.04 | −3.90±0.11 | −0.67±0.03 | 0.02 |

Table 5: Predicted intensity-averaged $MCL$ relations for He-burning fundamental pulsators with $Z$=0.02 and $Y$=0.25 to $Y$=0.31. The last column gives the intrinsic uncertainty $\epsilon_{MCL}(\log M_e)$ on the evolutionary mass inferred by these relations due to the above helium content variation and to the intrinsic dispersion, $\sigma$=0.04, in the adopted $ML$ relation. Note that $L_{can}$ is the luminosity of a given mass as based on B0 canonical evolutionary tracks (see text).

| $[CI]$ | $a$ | $b$ | $c$ | $d$ | $\epsilon_{MCL}(\log M_e)$ |
|---|---|---|---|---|---|
| | | $\langle M_V \rangle = a + b[CI] + c\log M/M_\odot + d\log(L/L_{can})$ | | | |
| $\langle M_B \rangle - \langle M_V \rangle$ | +2.42±0.11 | +0.82±0.06 | −8.35±0.11 | −2.66±0.08 | 0.03 |
| $\langle M_V \rangle - \langle M_R \rangle$ | +2.28±0.11 | +1.93±0.14 | −8.37±0.10 | −2.65±0.08 | 0.03 |
| $\langle M_V \rangle - \langle M_I \rangle$ | +2.24±0.11 | +1.07±0.08 | −8.37±0.10 | −2.64±0.08 | 0.02 |
| $\langle M_V \rangle - \langle M_J \rangle$ | +2.32±0.10 | +0.59±0.04 | −8.39±0.10 | −2.64±0.08 | 0.02 |
| $\langle M_V \rangle - \langle M_K \rangle$ | +2.33±0.10 | +0.43±0.03 | −8.39±0.10 | −2.63±0.07 | 0.02 |

Table 6: Estimated effects on $M_p$ and $M_e$ determinations due to variations in the pulsation period, the metal content, the true distance modulus, and the reddening.

| Pulsation mass | | | | | |
|---|---|---|---|---|---|
| $\partial \log M_p /$ | $\log L/L_{can}$ | $\partial \log P$ | $\log(Z/0.02)$ | $\partial \mu_0$ | $\partial E(B-V)$ |
| $PLC(BV)$ | – | $-1.33$ | $-0.35$ | $+0.48$ | $+0.36$ |
| $PLC(VI)$ | – | $-1.19$ | $+0.02$ | $+0.44$ | $-0.36$ |
| $PLC(VJ)$ | – | $-1.14$ | $+0.02$ | $+0.42$ | $-0.40$ |
| $PLC(VK)$ | – | $-1.07$ | $+0.02$ | $+0.41$ | $-0.16$ |
| Evolutionary mass | | | | | |
| $\partial \log M_e /$ | $\log L/L_{can}$ | $\partial \log P$ | $\log(Z/0.02)$ | $\partial \mu_0$ | $\partial E(B-V)$ |
| $MPL(V)$ | $-0.32$ | $+0.07$ | $+0.01$ | $+0.11$ | $+0.36$ |
| $MPL(I)$ | $-0.29$ | $-0.06$ | $+0.01$ | $+0.14$ | $+0.28$ |
| $MPL(J)$ | $-0.25$ | $-0.24$ | $+0.01$ | $+0.19$ | $+0.15$ |
| $MPL(K)$ | $-0.17$ | $-0.50$ | $+0.01$ | $+0.26$ | $+0.08$ |
| | | | | | |
| $MCL(BV)$ | $-0.32$ | – | $+0.01$ | $+0.12$ | $+0.30$ |
| $MCL(VI)$ | $-0.32$ | – | $+0.01$ | $+0.12$ | $+0.23$ |
| $MCL(VJ)$ | $-0.31$ | – | $+0.01$ | $+0.12$ | $+0.22$ |
| $MCL(VK)$ | $-0.31$ | – | $+0.01$ | $+0.12$ | $+0.24$ |

Table 7: Pulsation masses (solar units) of Milky Way Cepheids derived using predicted $PLC$ relations with $Z$=0.02 and $Y$=0.25 to 0.31. The errors in the last column refer to $VI$, $VJ$, and $VK$-based estimates.

| name | log$P$ | $M_V$ | log$M_p$ $\langle BV\rangle$ | er | log$M_p$ $\langle VI\rangle$ | log$M_p$ $\langle VJ\rangle$ | log$M_p$ $\langle VK\rangle$ | er |
|---|---|---|---|---|---|---|---|---|
| SU Cas | 0.2899 | −3.140 | 0.856 | 0.045 | 0.826 | 0.847 | 0.817 | 0.034 |
| EV Sct | 0.4901 | −3.345 | 0.749 | 0.058 | 0.861 | 0.779 | 0.737 | 0.048 |
| BF Oph | 0.6093 | −2.750 | 0.488 | 0.034 | 0.479 | 0.542 | 0.534 | 0.022 |
| T Vel | 0.6665 | −2.692 | 0.418 | 0.041 | 0.427 | 0.526 | 0.518 | 0.030 |
| $\delta$ Cep | 0.7297 | −3.431 | 0.585 | 0.037 | 0.61 | 0.655 | 0.656 | 0.025 |
| CV Mon | 0.7307 | −3.038 | 0.417 | 0.034 | 0.615 | 0.621 | 0.611 | 0.022 |
| V Cen | 0.7399 | −3.295 | 0.531 | 0.042 | 0.583 | 0.643 | 0.638 | 0.031 |
| BB Sgr | 0.8220 | −3.518 | 0.672 | 0.033 | 0.698 | 0.707 | 0.696 | 0.020 |
| U Sgr | 0.8290 | −3.477 | 0.633 | 0.032 | 0.660 | 0.671 | 0.653 | 0.019 |
| $\eta$ Aql | 0.8559 | −3.581 | 0.577 | 0.037 | 0.61 | 0.645 | 0.639 | 0.025 |
| S Nor | 0.9892 | −4.101 | 0.793 | 0.034 | 0.771 | 0.840 | 0.822 | 0.021 |
| XX Cen | 1.0395 | −4.154 | 0.713 | 0.032 | 0.718 | 0.770 | 0.755 | 0.020 |
| V340 Nor | 1.0526 | −3.814 | 0.661 | 0.093 | 0.722 | 0.719 | 0.707 | 0.020 |
| UU Mus | 1.0658 | −4.159 | 0.691 | 0.050 | 0.722 | 0.796 | 0.778 | 0.039 |
| U Nor | 1.1019 | −4.415 | 0.727 | 0.041 | 0.735 | 0.787 | 0.771 | 0.030 |
| BN Pup | 1.1359 | −4.513 | 0.784 | 0.038 | 0.781 | 0.817 | 0.809 | 0.027 |
| LS Pup | 1.1506 | −4.685 | 0.860 | 0.040 | 0.827 | 0.874 | 0.865 | 0.029 |
| VW Cen | 1.1771 | −4.037 | 0.675 | 0.035 | 0.713 | 0.804 | 0.786 | 0.023 |
| X Cyg | 1.2145 | −4.991 | 1.052 | 0.031 | 0.926 | 0.941 | 0.935 | 0.020 |
| VY Car | 1.2768 | −4.846 | 0.959 | 0.032 | 0.897 | 0.951 | 0.928 | 0.020 |
| RY Sco | 1.3079 | −5.060 | 0.716 | 0.034 | 0.802 | 0.811 | 0.794 | 0.022 |
| RZ Vel | 1.3096 | −5.042 | 0.858 | 0.033 | 0.845 | 0.916 | 0.897 | 0.021 |
| WZ Sgr | 1.3394 | −4.801 | 0.866 | 0.037 | 0.892 | 0.934 | 0.915 | 0.026 |
| WZ Car | 1.3620 | −4.918 | 0.710 | 0.043 | 0.750 | 0.831 | 0.811 | 0.033 |
| VZ Pup | 1.3649 | −5.009 | 0.643 | 0.040 | 0.665 | 0.704 | 0.703 | 0.029 |
| SW Vel | 1.3700 | −5.019 | 0.786 | 0.032 | 0.820 | 0.880 | 0.866 | 0.020 |
| T Mon | 1.4319 | −5.372 | 1.066 | 0.040 | 0.971 | 1.028 | 1.01 | 0.029 |
| RY Vel | 1.4492 | −5.501 | 0.909 | 0.034 | 0.905 | 0.965 | 0.93 | 0.021 |
| AQ Pup | 1.4786 | −5.513 | 0.944 | 0.037 | 1.004 | 0.974 | 0.961 | 0.025 |
| KN Cen | 1.5319 | −6.328 | 1.045 | 0.037 | 0.958 | 1.072 | 1.095 | 0.025 |
| l Car | 1.5509 | −5.821 | 1.290 | 0.034 | 1.133 | 1.165 | 1.137 | 0.021 |
| U Car | 1.5891 | −5.617 | 0.880 | 0.034 | 0.876 | 0.929 | 0.911 | 0.021 |
| RS Pup | 1.6174 | −6.015 | 1.123 | 0.043 | 1.134 | 1.136 | 1.107 | 0.032 |
| SV Vul | 1.6532 | −6.752 | 1.315 | 0.035 | 1.234 | 1.166 | 1.144 | 0.023 |

Table 8: Evolutionary masses (solar units) of Milky Way Cepheids, derived using predicted $MPL$ relations based on canonical evolutionary tracks with $Z$=0.02 and $Y$=0.28±0.03.

| name | log$P$ | $M_V$ | log$M_e(V)$ | log$M_e(I)$ | log$M_e(J)$ | log$M_e(K)$ | er |
|---|---|---|---|---|---|---|---|
| SU Cas | 0.2899 | −3.140 | 0.712 | 0.723 | 0.745 | 0.761 | 0.030 |
| EV Sct | 0.4901 | −3.345 | 0.748 | 0.759 | 0.754 | 0.739 | 0.033 |
| BF Oph | 0.6093 | −2.750 | 0.691 | 0.670 | 0.653 | 0.612 | 0.027 |
| T Vel | 0.6665 | −2.692 | 0.689 | 0.663 | 0.648 | 0.604 | 0.029 |
| $\delta$ Cep | 0.7297 | −3.431 | 0.774 | 0.757 | 0.743 | 0.713 | 0.028 |
| CV Mon | 0.7307 | −3.038 | 0.731 | 0.720 | 0.703 | 0.671 | 0.027 |
| V Cen | 0.7399 | −3.295 | 0.760 | 0.742 | 0.730 | 0.698 | 0.029 |
| BB Sgr | 0.8220 | −3.518 | 0.789 | 0.780 | 0.768 | 0.742 | 0.027 |
| U Sgr | 0.8290 | −3.477 | 0.785 | 0.773 | 0.756 | 0.718 | 0.027 |
| $\eta$ Aql | 0.8559 | −3.581 | 0.799 | 0.779 | 0.759 | 0.718 | 0.028 |
| S Nor | 0.9892 | −4.101 | 0.864 | 0.855 | 0.858 | 0.842 | 0.027 |
| XX Cen | 1.0395 | −4.154 | 0.873 | 0.857 | 0.846 | 0.812 | 0.027 |
| V340 Nor | 1.0526 | −3.814 | 0.837 | 0.826 | 0.807 | 0.772 | 0.044 |
| UU Mus | 1.0658 | −4.159 | 0.876 | 0.860 | 0.855 | 0.826 | 0.031 |
| U Nor | 1.1019 | −4.415 | 0.906 | 0.888 | 0.875 | 0.836 | 0.029 |
| BN Pup | 1.1359 | −4.513 | 0.919 | 0.905 | 0.892 | 0.862 | 0.028 |
| LS Pup | 1.1506 | −4.685 | 0.939 | 0.927 | 0.921 | 0.899 | 0.029 |
| VW Cen | 1.1771 | −4.037 | 0.870 | 0.855 | 0.854 | 0.829 | 0.027 |
| X Cyg | 1.2145 | −4.991 | 0.976 | 0.971 | 0.966 | 0.953 | 0.027 |
| VY Car | 1.2768 | −4.846 | 0.965 | 0.958 | 0.961 | 0.945 | 0.027 |
| RY Sco | 1.3079 | −5.060 | 0.990 | 0.971 | 0.943 | 0.888 | 0.027 |
| RZ Vel | 1.3096 | −5.042 | 0.988 | 0.973 | 0.969 | 0.940 | 0.027 |
| WZ Sgr | 1.3394 | −4.801 | 0.964 | 0.957 | 0.956 | 0.939 | 0.028 |
| WZ Car | 1.3620 | −4.918 | 0.978 | 0.955 | 0.940 | 0.893 | 0.029 |
| VZ Pup | 1.3649 | −5.009 | 0.989 | 0.955 | 0.914 | 0.842 | 0.029 |
| SW Vel | 1.3700 | −5.019 | 0.990 | 0.972 | 0.961 | 0.926 | 0.027 |
| T Mon | 1.4319 | −5.372 | 1.032 | 1.026 | 1.031 | 1.019 | 0.029 |
| RY Vel | 1.4492 | −5.501 | 1.048 | 1.033 | 1.025 | 0.985 | 0.027 |
| AQ Pup | 1.4786 | −5.513 | 1.051 | 1.046 | 1.030 | 1.003 | 0.028 |
| KN Cen | 1.5319 | −6.328 | 1.143 | 1.123 | 1.122 | 1.113 | 0.028 |
| l Car | 1.5509 | −5.821 | 1.089 | 1.093 | 1.108 | 1.111 | 0.027 |
| U Car | 1.5891 | −5.617 | 1.070 | 1.050 | 1.033 | 0.987 | 0.027 |
| RS Pup | 1.6174 | −6.015 | 1.115 | 1.116 | 1.119 | 1.108 | 0.029 |
| SV Vul | 1.6532 | −6.752 | 1.197 | 1.200 | 1.186 | 1.164 | 0.027 |

Table 9: Evolutionary masses (solar units) of Milky Way Cepheids, derived using predicted $MCL$ relations based on canonical evolutionary tracks with $Z$=0.02 and $Y$=0.28±0.03.

| name | log$P$ | $M_V$ | log$M_e(BV)$ | log$M_e(VI)$ | log$M_e(VJ)$ | log$M_e(VK)$ | er |
|---|---|---|---|---|---|---|---|
| SU Cas | 0.2899 | −3.140 | 0.706 | 0.704 | 0.706 | 0.703 | 0.027 |
| EV Sct | 0.4901 | −3.345 | 0.735 | 0.745 | 0.737 | 0.733 | 0.029 |
| BF Oph | 0.6093 | −2.750 | 0.679 | 0.676 | 0.681 | 0.679 | 0.025 |
| T Vel | 0.6665 | −2.692 | 0.675 | 0.673 | 0.681 | 0.679 | 0.026 |
| $\delta$ Cep | 0.7297 | −3.431 | 0.755 | 0.755 | 0.758 | 0.758 | 0.026 |
| CV Mon | 0.7307 | −3.038 | 0.709 | 0.725 | 0.725 | 0.723 | 0.025 |
| V Cen | 0.7399 | −3.295 | 0.741 | 0.743 | 0.748 | 0.747 | 0.026 |
| BB Sgr | 0.8220 | −3.518 | 0.779 | 0.780 | 0.780 | 0.779 | 0.025 |
| U Sgr | 0.8290 | −3.477 | 0.773 | 0.774 | 0.775 | 0.772 | 0.025 |
| $\eta$ Aql | 0.8559 | −3.581 | 0.780 | 0.781 | 0.783 | 0.782 | 0.026 |
| S Nor | 0.9892 | −4.101 | 0.854 | 0.851 | 0.857 | 0.855 | 0.025 |
| XX Cen | 1.0395 | −4.154 | 0.857 | 0.856 | 0.860 | 0.858 | 0.025 |
| V340 Nor | 1.0526 | −3.814 | 0.827 | 0.831 | 0.830 | 0.828 | 0.035 |
| UU Mus | 1.0658 | −4.159 | 0.859 | 0.859 | 0.866 | 0.864 | 0.027 |
| U Nor | 1.1019 | −4.415 | 0.886 | 0.885 | 0.889 | 0.887 | 0.026 |
| BN Pup | 1.1359 | −4.513 | 0.903 | 0.901 | 0.903 | 0.902 | 0.026 |
| LS Pup | 1.1506 | −4.685 | 0.924 | 0.920 | 0.924 | 0.922 | 0.026 |
| VW Cen | 1.1771 | −4.037 | 0.860 | 0.861 | 0.869 | 0.867 | 0.026 |
| X Cyg | 1.2145 | −4.991 | 0.972 | 0.960 | 0.961 | 0.960 | 0.025 |
| VY Car | 1.2768 | −4.846 | 0.959 | 0.953 | 0.958 | 0.955 | 0.025 |
| RY Sco | 1.3079 | −5.060 | 0.960 | 0.964 | 0.964 | 0.961 | 0.025 |
| RZ Vel | 1.3096 | −5.042 | 0.970 | 0.967 | 0.973 | 0.971 | 0.025 |
| WZ Sgr | 1.3394 | −4.801 | 0.955 | 0.956 | 0.960 | 0.957 | 0.026 |
| WZ Car | 1.3620 | −4.918 | 0.954 | 0.954 | 0.961 | 0.958 | 0.026 |
| VZ Pup | 1.3649 | −5.009 | 0.956 | 0.954 | 0.956 | 0.954 | 0.026 |
| SW Vel | 1.3700 | −5.019 | 0.969 | 0.970 | 0.975 | 0.972 | 0.025 |
| T Mon | 1.4319 | −5.372 | 1.027 | 1.018 | 1.023 | 1.021 | 0.026 |
| RY Vel | 1.4492 | −5.501 | 1.027 | 1.024 | 1.029 | 1.025 | 0.025 |
| AQ Pup | 1.4786 | −5.513 | 1.034 | 1.038 | 1.034 | 1.032 | 0.026 |
| KN Cen | 1.5319 | −6.328 | 1.114 | 1.103 | 1.113 | 1.115 | 0.026 |
| U Car | 1.5891 | −5.617 | 1.049 | 1.046 | 1.050 | 1.047 | 0.025 |
| l Car | 1.5509 | −5.821 | 1.095 | 1.082 | 1.085 | 1.082 | 0.025 |
| RS Pup | 1.6174 | −6.015 | 1.104 | 1.104 | 1.105 | 1.101 | 0.026 |
| SV Vul | 1.6532 | −6.752 | 1.183 | 1.176 | 1.169 | 1.166 | 0.025 |

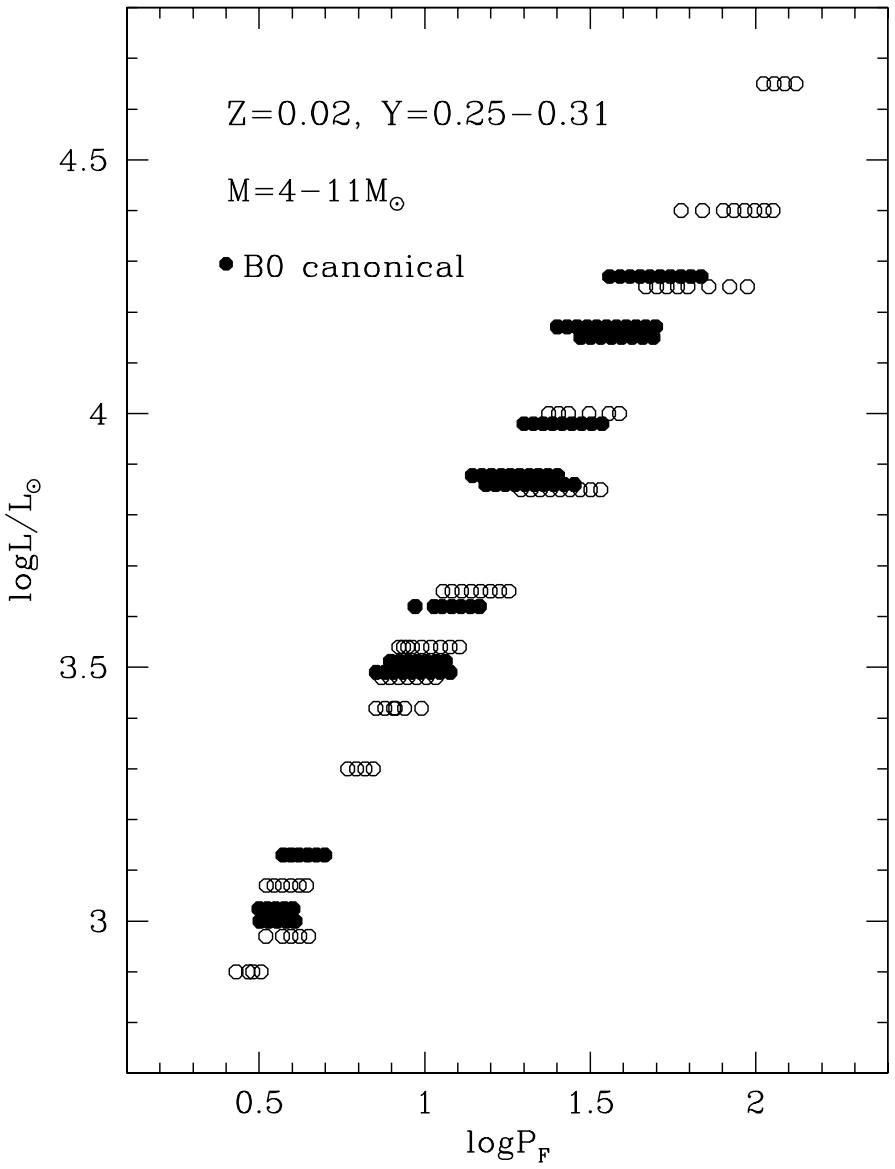


Fig. 1.— Period-Luminosity distribution of fundamental pulsators with fixed metal content ($Z$=0.02) and helium abundance ranging from $Y$=0.25 to 0.31. Filled dots display Cepheid models computed by adopting the Bono et al. (2000) canonical $ML$ relation.

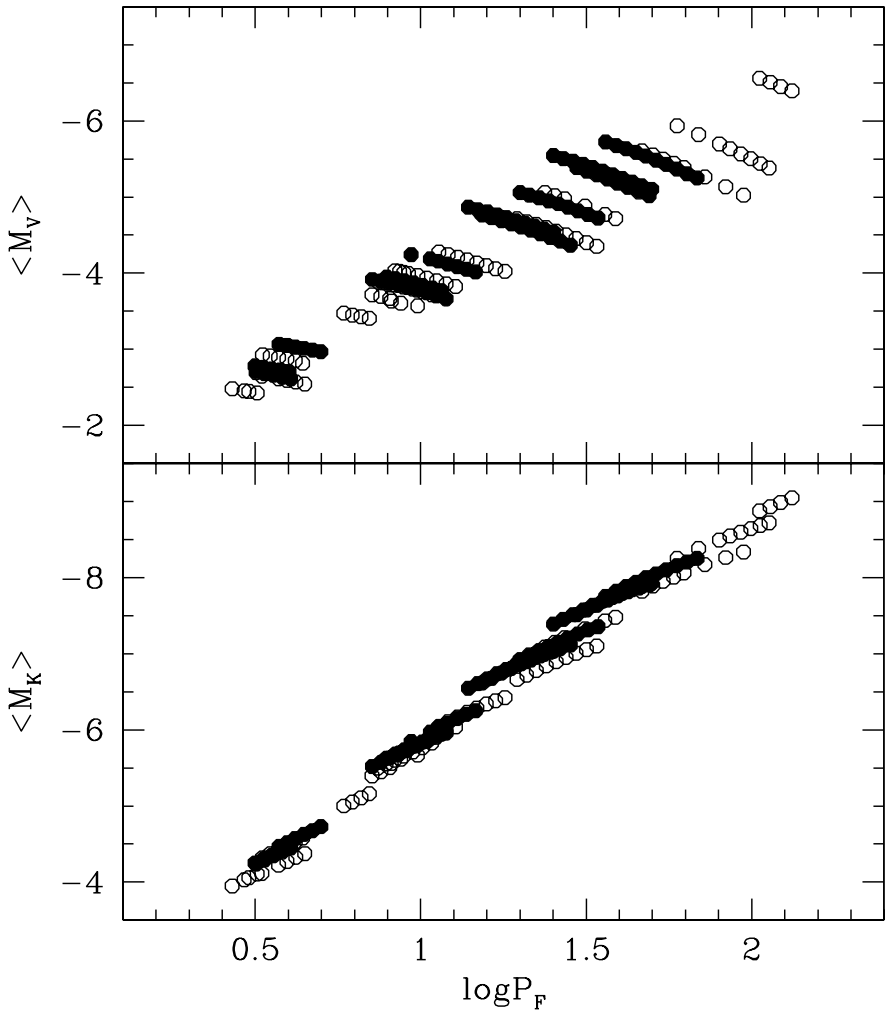


Fig. 2.— Same as in Fig. 1, but for the Period-Magnitude distribution in V and K photometric bands.

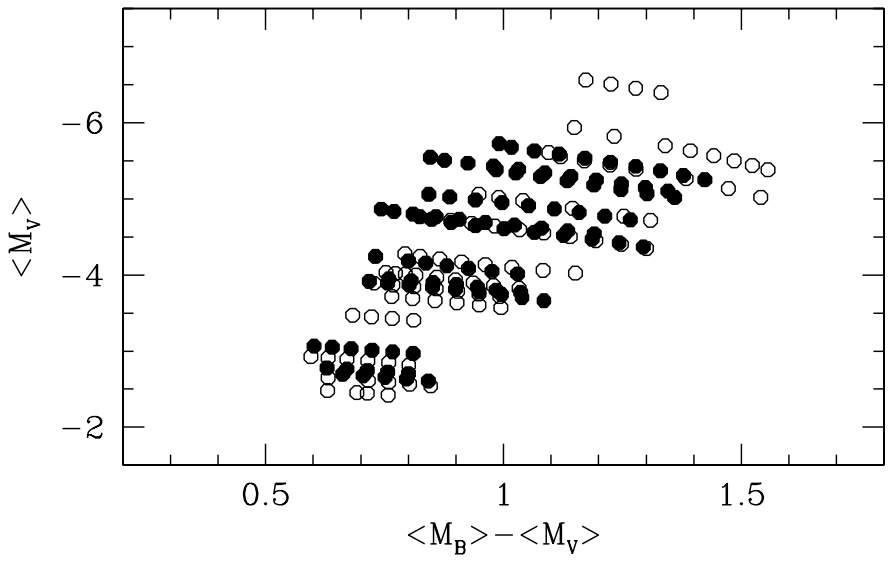


Fig. 3.— Distribution of the fundamental pulsators in the Color-Magnitude diagram. Symbols are the same as in Figure 1.

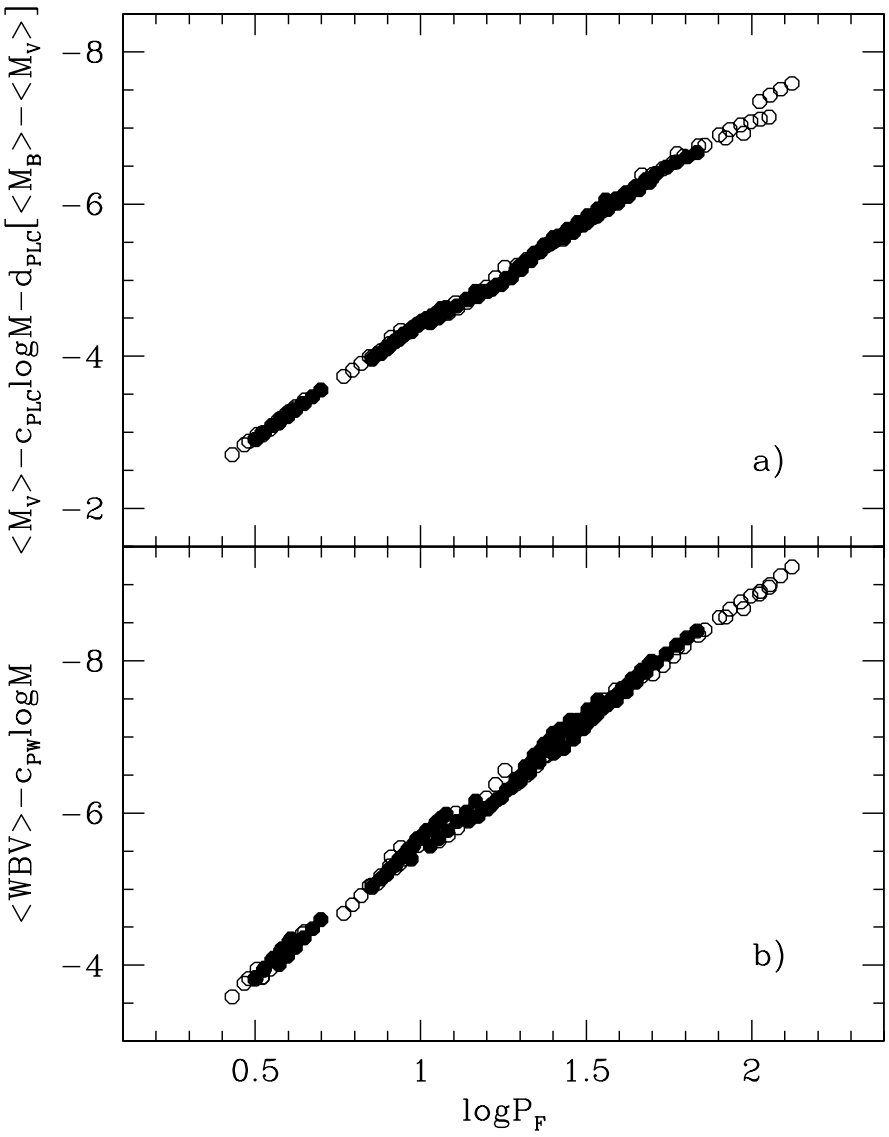


Fig. 4.— Panel a) - Predicted $PLC(BV)$ relation for the fundamental pulsators plotted in Fig. 1. Panel b) - Same as the top, but for predicted Period-$\langle WBV \rangle$ relation.

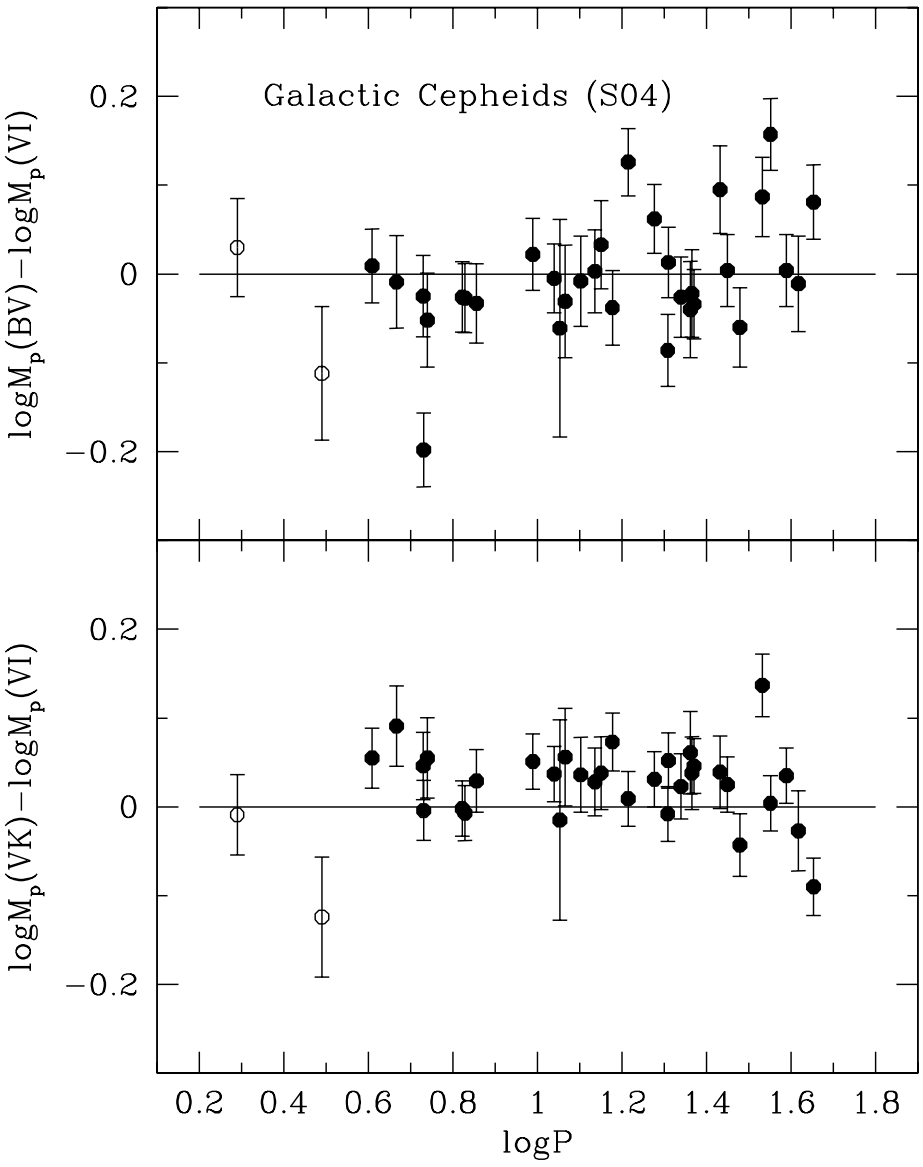


Fig. 5.— Top panel - Difference in the pulsation masses of Galactic Cepheids estimated using optical $(B-V, V-I)$ $PLC$ relations. Bottom panel - Same as the top, but for $PLC$ relations based on $V-K$ and $V-I$) colors

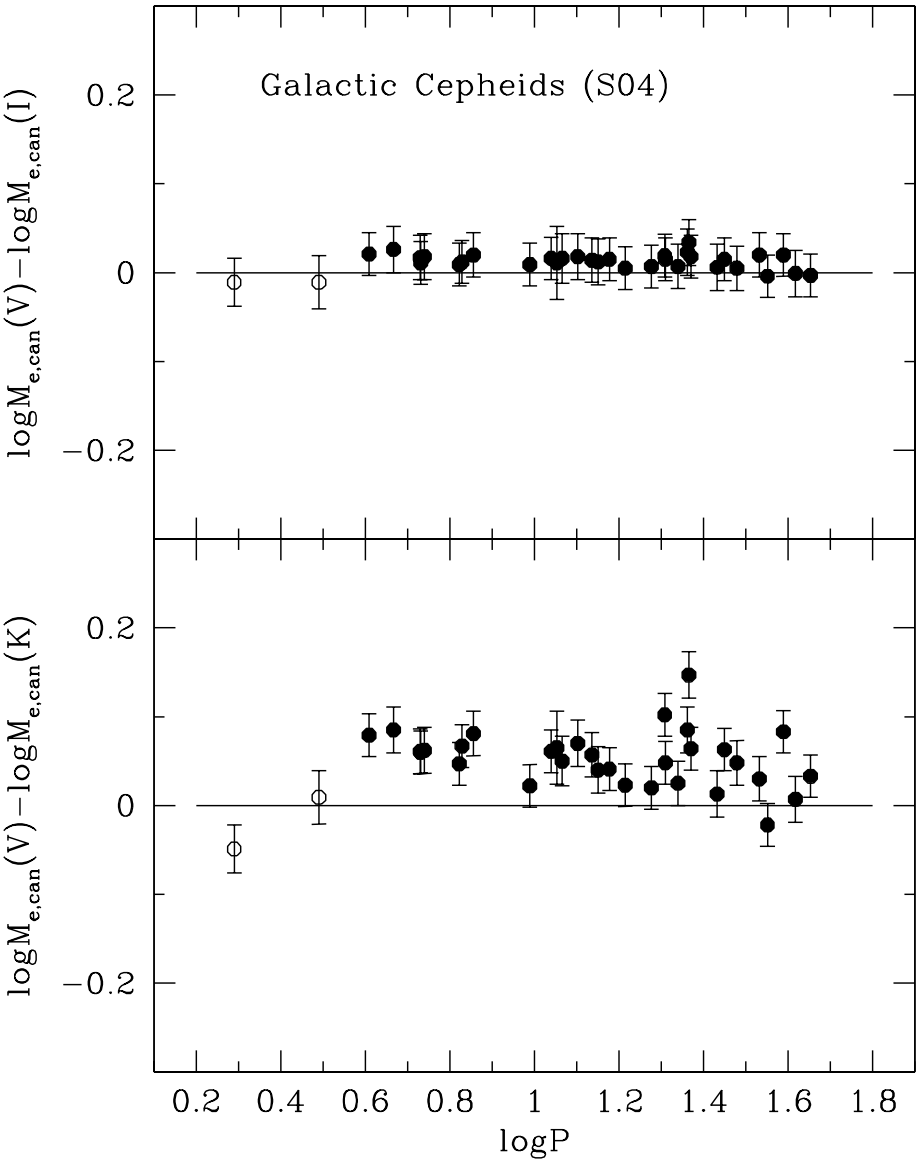


Fig. 6.— Top panel - Difference in the the canonical evolutionary masses of Galactic Cepheids estimated using $V$ and $I$-band $MPL$ relations. Bottom panel - Same as the top, but for $MPL$ relations based on $V$ and $K$ magnitudes.

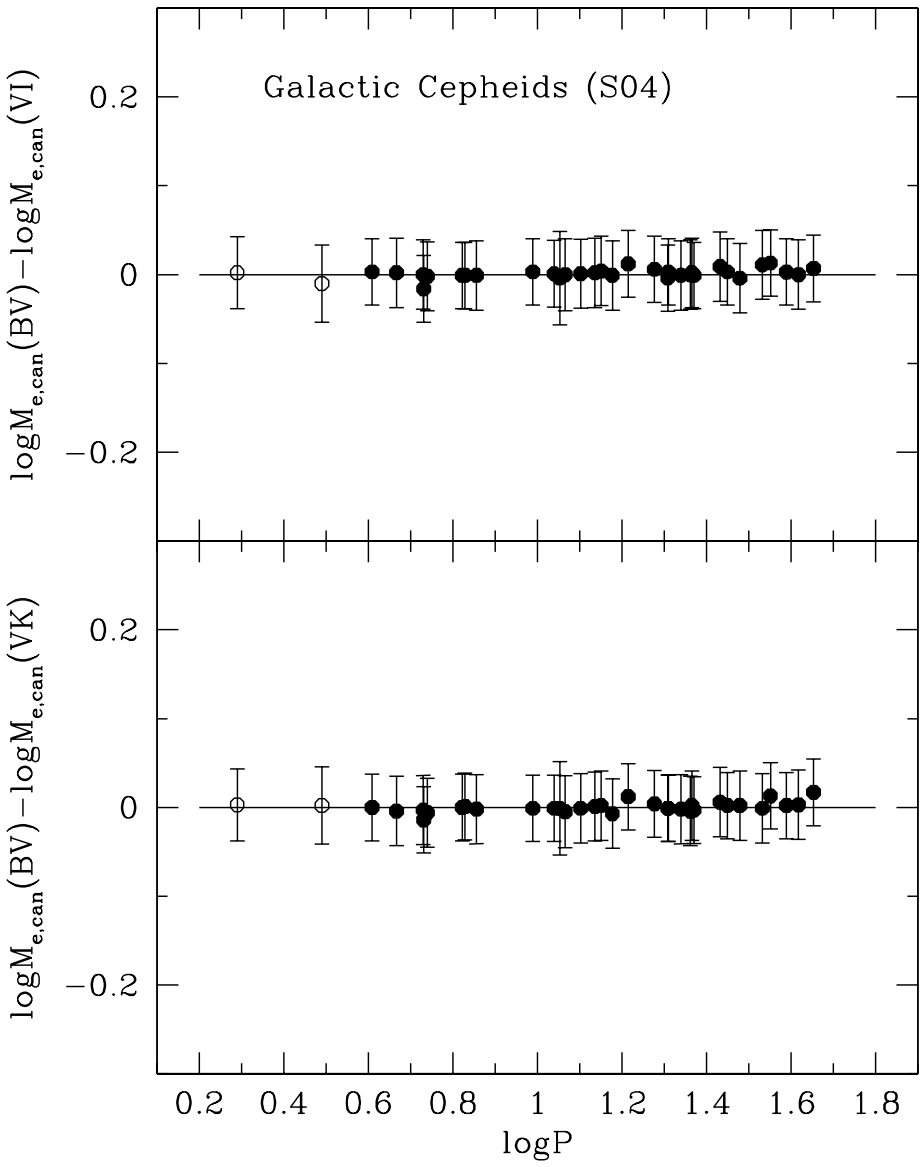


Fig. 7.— Top panel - Difference in the the canonical evolutionary masses of Galactic Cepheids estimated using optical ($B-V$, $V-I$) $MCL$ relations. Bottom panel - Same as the top, but for $MCL$ relations based on $B-V$ and $V-K$ colors.

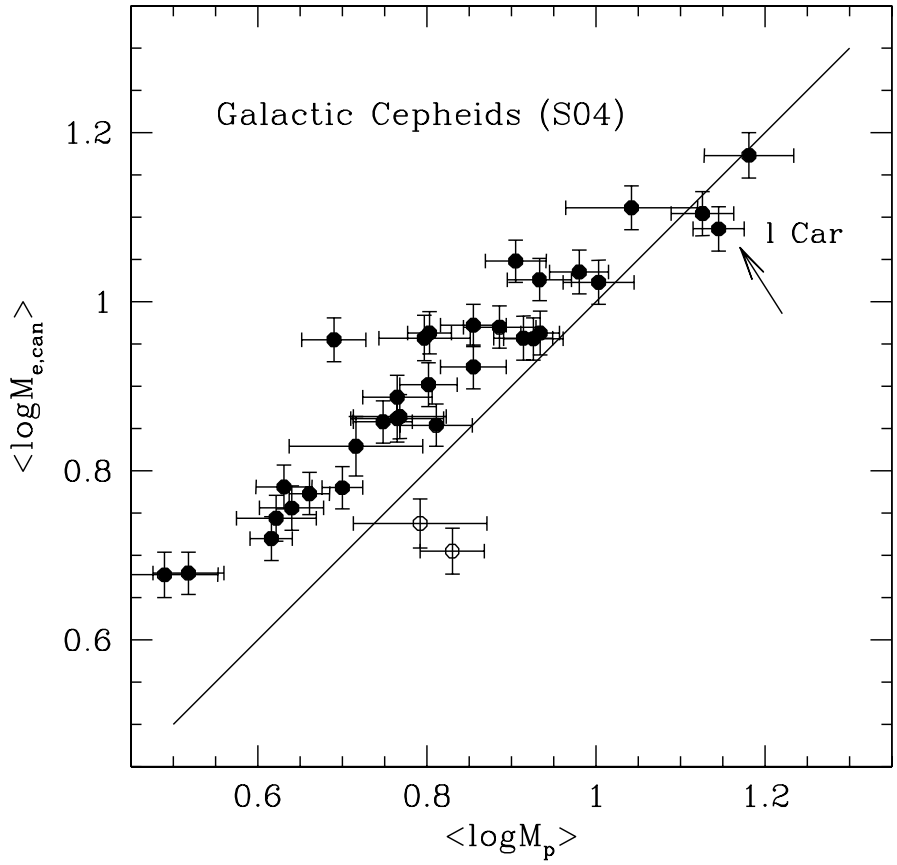


Fig. 8.— Mean pulsation mass of Galactic Cepheids versus the mean canonical evolutionary one. Open dots mark the short-period Cepheids SU Cas and EV Sct, while the small arrow marks the long-period variable l Car.

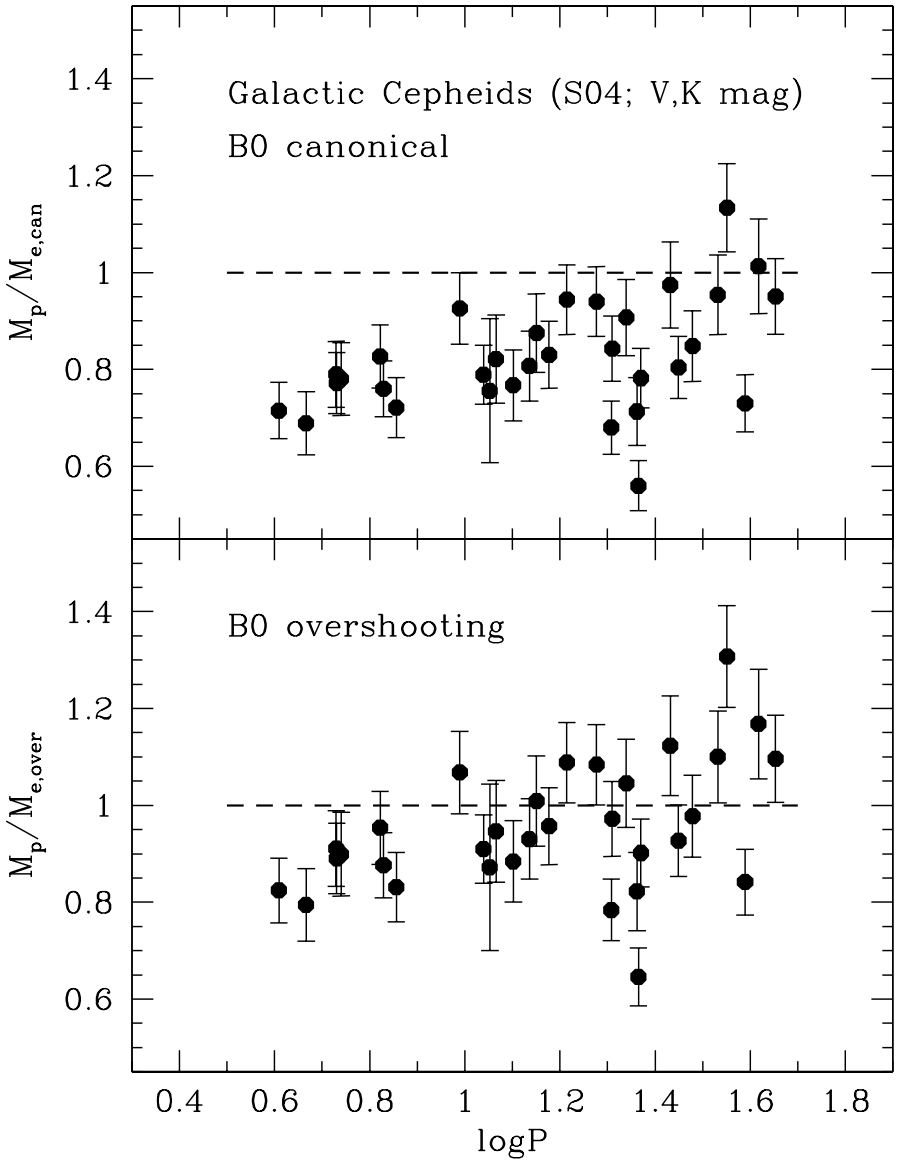


Fig. 9.— Top panel: Ratio between pulsation and canonical evolutionary mass for Galactic Cepheids as a function of period. The two estimates are based on $V, K$ magnitudes. Bottom panel: Same as the top, but for evolutionary models whose luminosity was artificially increased to account for convective core overshooting. See text for more details.

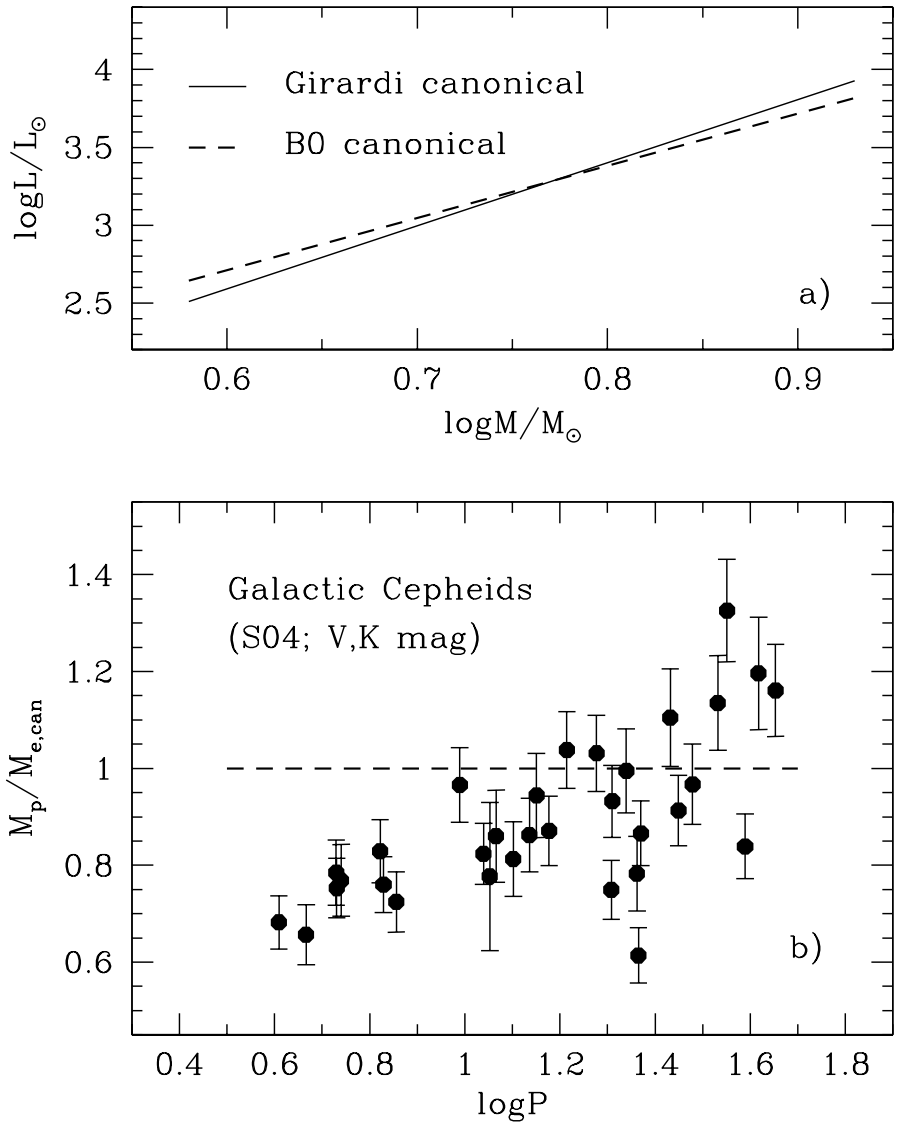


Fig. 10.— Panel a) - Comparison between the canonical $ML$ relation adopted in this investigation (dashed line) and the $ML$ relation for canonical evolutionary models (solid line) provided by Girardi et al. (2000). Panel b) - Same as the top panel of Fig. 9, but based on Girardi et al. (2000) canonical evolutionary computations.

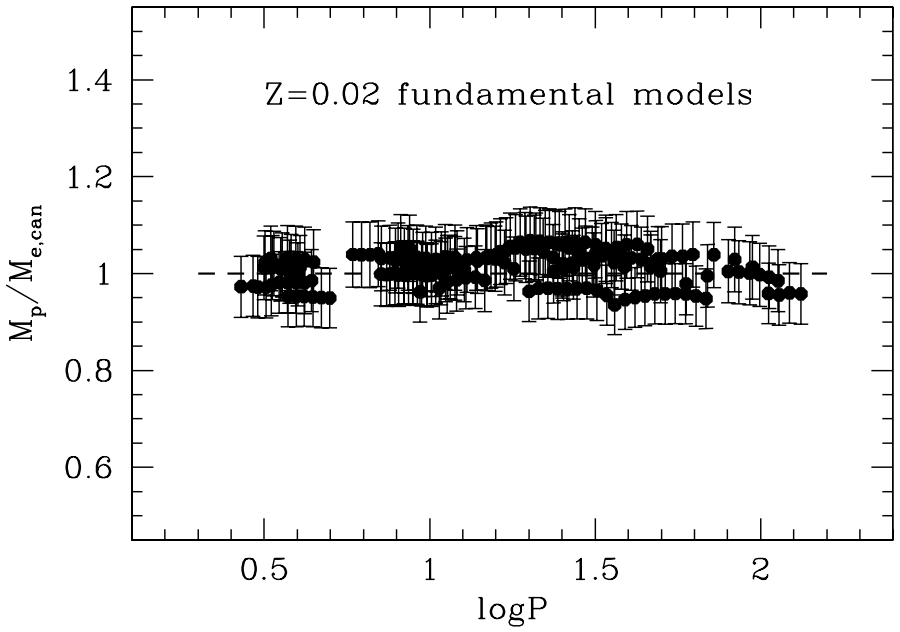


Fig. 11.— Same as the top panel of Fig. 9, but for the fundamental pulsation models listed in Table 1.

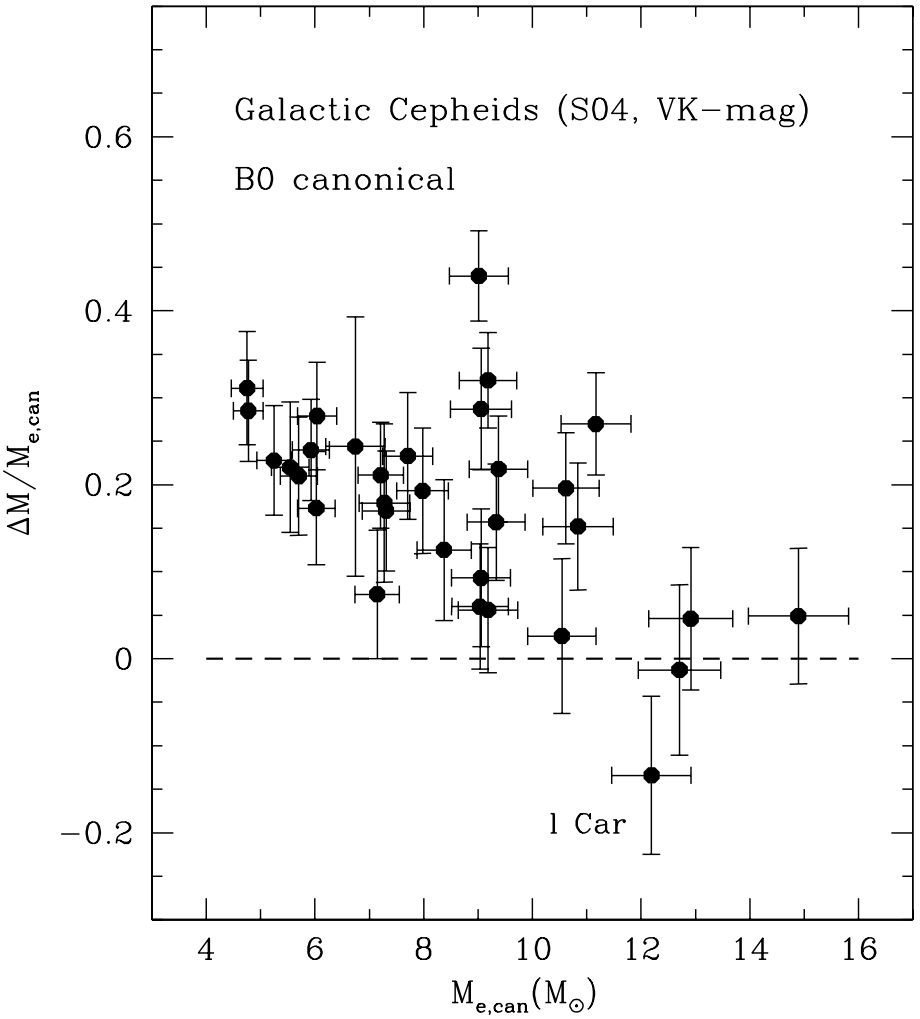


Fig. 12.— Relative difference between pulsation ($M_p$) and canonical evolutionary mass ($\Delta M = M_{e,can} - M_p$) as a function of the canonical evolutionary mass for Galactic Cepheids.